
Clustering Complex Excitations in Linear Arrays with Hilbert Ordering

A. Benoni, P. Rocca, N. Anselmi, and A. Massa

2024/06/14

Contents

1 Numerical Results	3
1.1 Perfomance Analysis	3
1.1.1 Flat Top Pattern, $N = [10, 25]$, $Q = [5, 10]$ - rotated excitations $\alpha \in [0, 360]$ [deg], $\Delta\alpha = 4$ [deg]	3
1.1.2 Cosecant Squared Pattern, $N = [10, 25]$, $Q = [5, 10]$ - rotated excitations $\alpha \in [0, 360]$ [deg], $\Delta\alpha = 4$ [deg]	8
1.1.3 Hibert Curve Sorting + Exhaustive Search (Excitation Matching): Comparison	15
1.1.4 Hibert Sorting + Exhaustive Search (Pattern Matching) vs K-means (Best Seed Excitation Matching)	18
1.1.5 Hibert Curve Sorting + Exhaustive Search (Pattern Matching) vs K-means (Best Seed Pattern Matching)	26
1.1.6 Hibert Curve Sorting + Swap Element Algorithm: Comparison Pattern Matching (Cost Function: Excitation Matching)	30

1 Numerical Results

1.1 Performace Analysis

1.1.1 Flat Top Pattern, $N = [10, 25]$, $Q = [5, 10]$ - rotated excitations $\alpha \in [0, 360]$ [deg], $\Delta\alpha = 4$ [deg]

Test Case Description

Antenna configuration

- isotropic elements
- number of elements: $N = [10, 25]$
- distance between elements along x axis: $d_x = \lambda/2$

Target excitations

- $w_n = \alpha_n e^{j\varphi_n}$ with $n = 1,..,N$
- Flat top

Sub-array generation

- number of clusters: $Q = [5, 10]$
- number realization: $R = 92$
- excitation matching strategies:
 - K-Means
 - * initialization: $R = 92$ random seeds
 - Hilbert + Exhaustive Search:
 - * initialization: $R = 92$ excitations rotations, $\alpha = [0, 360]$ [deg]
 - * rotation step: $\Delta\alpha = 4$ [deg]

Hilbert Curve Sorting + Exhaustive Search vs. K-means

The following comparative assessment has been performed, computing five different orders of Hilbert curve.

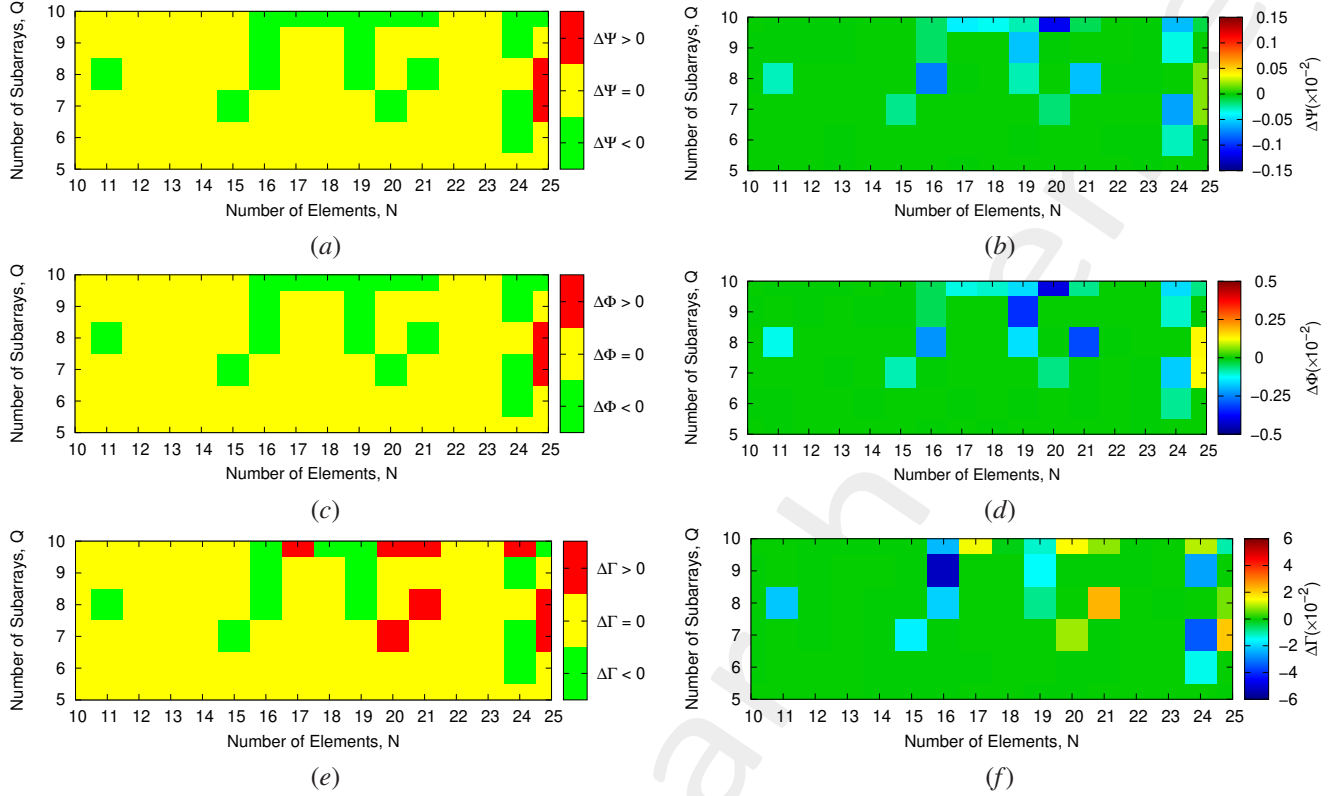


Figure 1: *Flat Top Pattern - rotated excitations [0, 360][deg]*, Performance Evaluation: (a)(c)(e) 3 colors map and (b)(d)(f) quantitative color map for the (a)(b) difference excitation matching, (c)(d) difference field matching and (e)(f) difference power pattern matching.

In the following a comparative assessment of the performance in terms of power pattern and subarray clusters. More in details, three configurations have been considered. For case $N = 20$ and $Q = 10$ the greatest improvement has been obtained compared to the K-means technique, while for case $N = 21$ and $Q = 10$ a slight improvement has been reached by the Hilbert Sorting. Instead, the third case ($N = 22$ and $Q = 10$) reports a configuration, where the two clustering approaches reach the same results in terms of excitation and field matching.

Number elements $N = 20$, **Number Clusters** $Q = 10$

- difference excitation matching: $\Delta\Psi = -1.15 \times 10^{-3}$
- difference field matching: $\Delta\Phi = -4.05 \times 10^{-3}$
- difference power pattern matching: $\Delta\Gamma = 1.47 \times 10^{-2}$

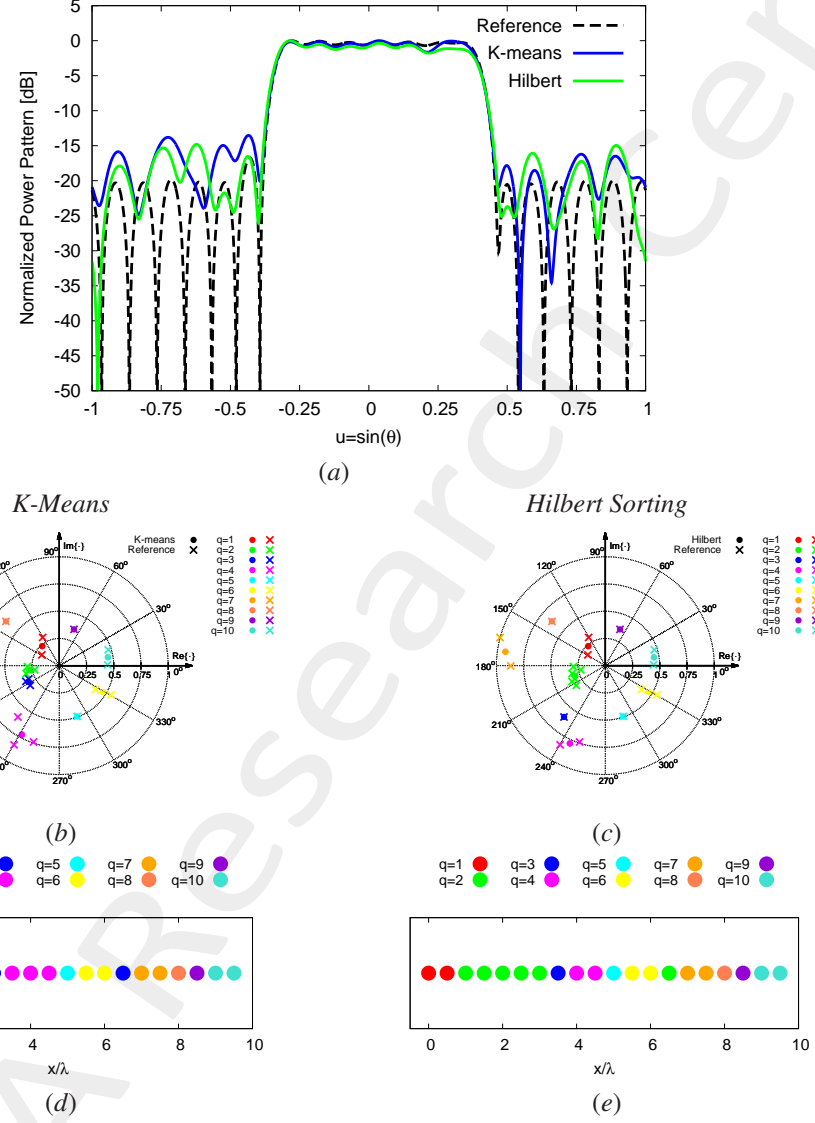


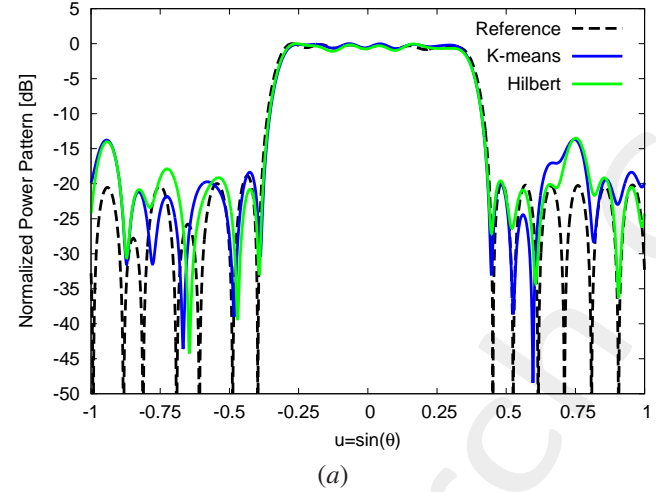
Figure 2: *Flat Top* ($N = 20$, $Q = 10$): plot of (a) the power pattern of the clusterized solutions computed with the K-Means (blue line) and the Hilbert Sorting (green line) together with the reference ones (dashed black line), (b)(c) representation of the reference and the sub-array excitations in the complex plane, and (d)(e) layout of the clustered array synthetized with (b)(d) the K-means and (c)(e) the Hilbert Sorting.

Method	Ψ	Φ	Γ	SLL [dB]	D [dBi]	$HPBW$ [u]
Hilbert Sorting	5.75×10^{-3}	2.020×10^{-2}	8.83×10^{-2}	-14.80	5.10	7.24×10^{-1}
K-Means	6.90×10^{-3}	2.425×10^{-2}	7.35×10^{-2}	-13.53	4.71	7.26×10^{-1}

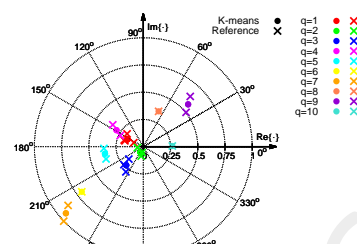
Table I: *Flat Top* ($N = 20$, $Q = 10$): values of excitation matching index, Ψ , the field matching index, Φ , the power pattern matching index, Γ , the SLL, the directivity D and the half power beamwidth $HPBW$ obtained with Hilbert Sorting + ES and with the K-means.

Number elements $N = 21$, **Number Clusters** $Q = 10$

- difference excitation matching: $\Delta\Psi = -1.26 \times 10^{-4}$
- difference field matching: $\Delta\Phi = -7.02 \times 10^{-4}$
- difference power pattern matching: $\Delta\Gamma = 8.31 \times 10^{-3}$



K-Means



Hilbert Sorting

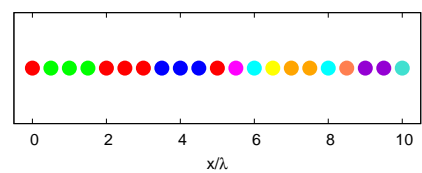
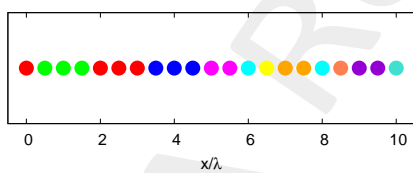
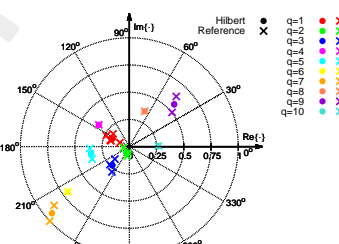


Figure 3: *Flat Top* ($N = 21$, $Q = 10$): plot of (a) the power pattern of the clusterized solutions computed with the K-Means (blue line) and the Hilbert Sorting (green line) together with the reference ones (dashed black line), (b)(c) representation of the reference and the sub-array excitations in the complex plane, and (d)(e) layout of the clustered array synthetized with (b)(d) the K-means and (c)(e) the Hilbert Sorting.

Method	Ψ	Φ	Γ	SLL [dB]	D [dBi]	$HPBW$ [u]
Hilbert Sorting	2.51×10^{-3}	1.377×10^{-2}	7.23×10^{-2}	-13.49	4.97	6.90×10^{-1}
K-Means	2.64×10^{-3}	1.447×10^{-2}	6.40×10^{-2}	-13.69	4.80	6.89×10^{-1}

Table II: *Flat Top* ($N = 21$, $Q = 10$): values of excitation matching index, Ψ , the field matching index, Φ , the power pattern matching index, Γ , the SLL, the directivity D and the half power beamwidth $HPBW$ obtained with Hilbert Sorting + ES and with the K-means.

Number elements $N = 22$, **Number Clusters** $Q = 10$

- difference excitation matching: $\Delta\Psi = -2.79 \times 10^{-9}$
- difference field matching: $\Delta\Phi = 0.00$
- difference power pattern matching: $\Delta\Gamma = 0.00$

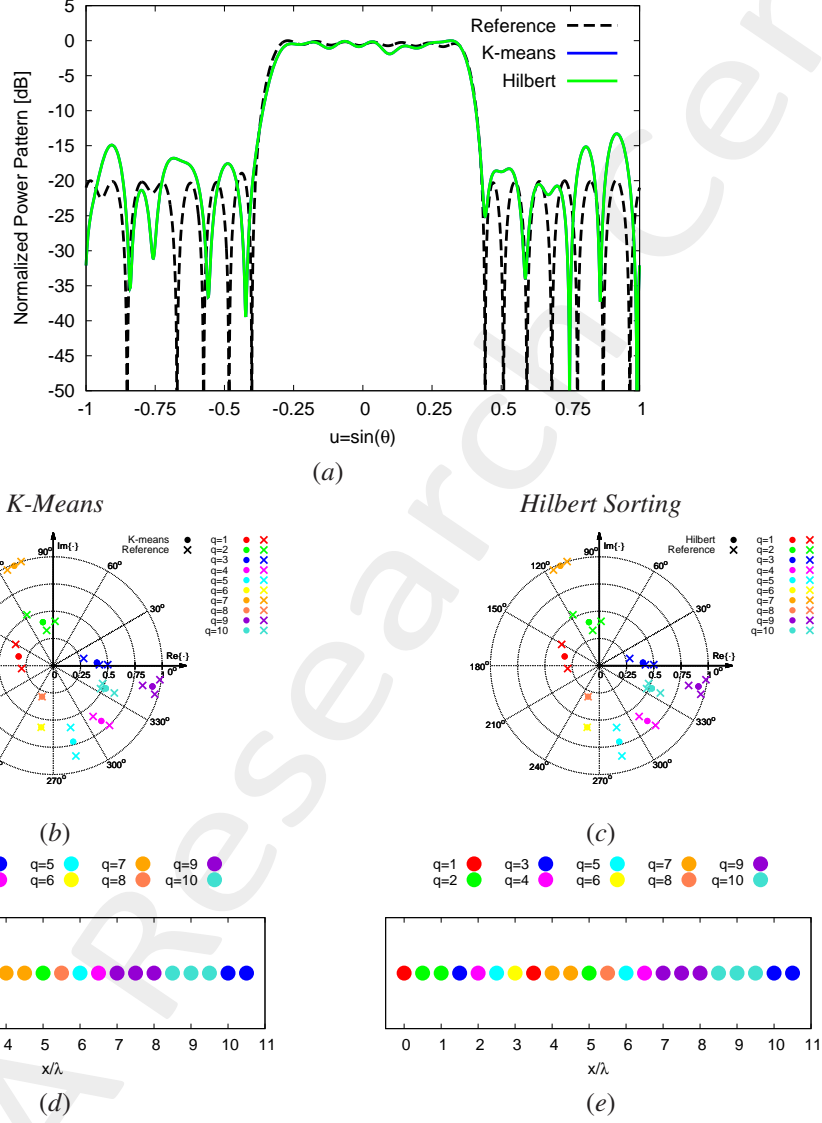


Figure 4: *Flat Top* ($N = 22$, $Q = 10$): plot of (a) the power pattern of the clusterized solutions computed with the K-Means (blue line) and the Hilbert Sorting (green line) together with the reference ones (dashed black line), (b)(c) representation of the reference and the sub-array excitations in the complex plane, and (d)(e) layout of the clustered array synthetized with (b)(d) the K-means and (c)(e) the Hilbert Sorting.

Method	Ψ	Φ	Γ	SLL [dB]	D [dBi]	$HPBW$ [u]
Hilbert Sorting	8.87×10^{-3}	2.139×10^{-3}	9.43×10^{-2}	-13.29	5.02	6.91×10^{-1}
K-Means	8.87×10^{-3}	2.139×10^{-3}	9.43×10^{-2}	-13.28	5.02	6.91×10^{-1}

Table III: *Flat Top* ($N = 22$, $Q = 10$): values of excitation matching index, Ψ , the field matching index, Φ , the power pattern matching index, Γ , the SLL, the directivity D and the half power beamwidth $HPBW$ obtained with Hilbert Sorting + ES and with the K-means.

1.1.2 Cosecant Squared Pattern, $N = [10, 25]$, $Q = [5, 10]$ - rotated excitations $\alpha \in [0, 360]$ [deg], $\Delta\alpha = 4$ [deg]

Test Case Description

Antenna configuration

- isotropic elements
- number of elements: $N = [10, 25]$
- distance between elements along x axis: $d_x = \lambda/2$

Target excitations

- $w_n = \alpha_n e^{j\varphi_n}$ with $n = 1, \dots, N$
- Cosecant Squared

Sub-array generation

- number of clusters: $Q = [5, 10]$
- number realization: $R = 92$
- excitation matching strategies:
 - K-Means
 - * initialization: $R = 92$ random seeds
 - Hilbert + Exhaustive Search:
 - * initialization: $R = 92$ excitations rotations, $\alpha = [0, 360]$ [deg]
 - * rotation step: $\Delta\alpha = 4$ [deg]

Hilbert Curve Sorting + Exhaustive Search vs. K-means

The following comparative assessment has been performed, computing five different orders of Hilbert curve.

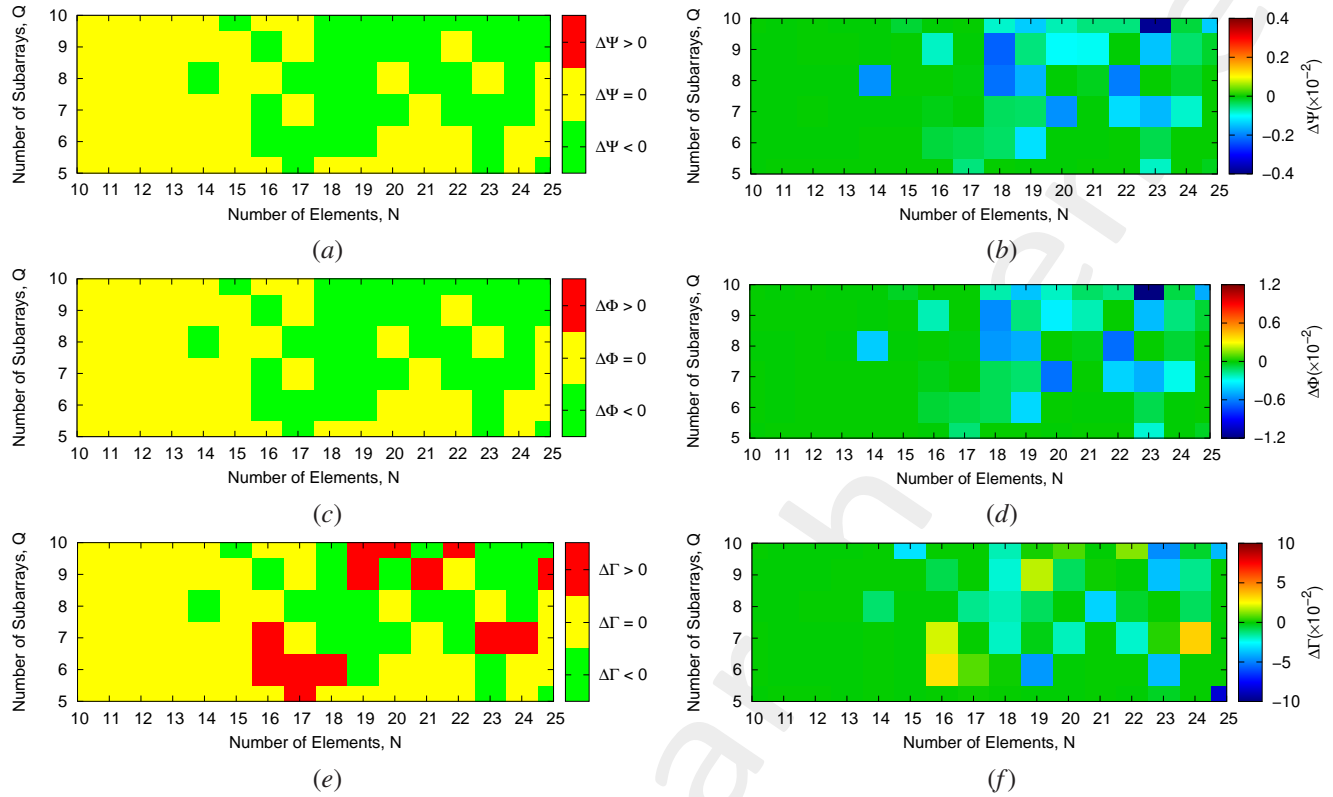
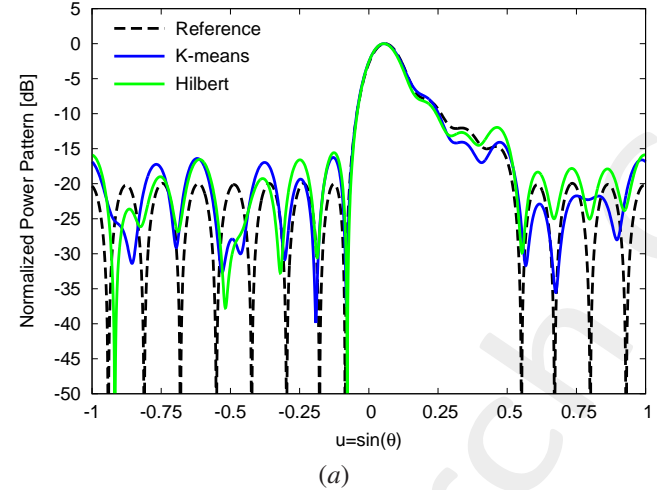


Figure 5: *Cosecant Squared Pattern - rotated excitations [0, 360][deg]*, Performance Evaluation: (a)(c)(e) 3 colors map and (b)(d)(f) quantitative color map for the (a)(b) difference excitation matching, (c)(d) difference field matching and (e)(f) difference power pattern matching.

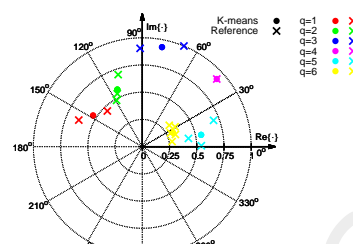
In the following a comparative assessment of the performance in terms of power pattern and subarray clusters for some case of interest.

Number elements $N = 16$, Number Clusters $Q = 6$

- difference excitation matching: $\Delta\Psi = -2.32 \times 10^{-4}$
- difference field matching: $\Delta\Phi = -6.23 \times 10^{-4}$
- difference power pattern matching: $\Delta\Gamma = 3.02 \times 10^{-2}$



K-Means



Hilbert Sorting

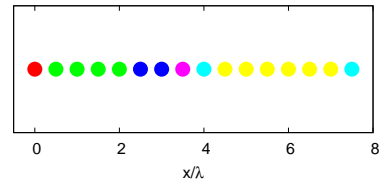
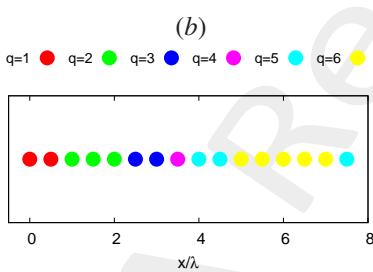
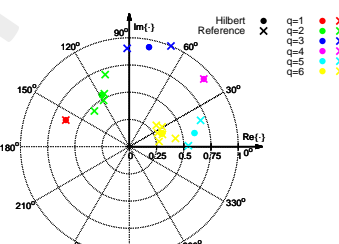


Figure 6: *Cosecant Squared* ($N = 16$, $Q = 6$): plot of (a) the power pattern of the clusterized solutions computed with the K-Means (blue line) and the Hilbert Sorting (green line) together with the reference ones (dashed black line), (b)(c) representation of the reference and the sub-array excitations in the complex plane, and (d)(e) layout of the clustered array synthetized with (b)(d) the K-means and (c)(e) the Hilbert Sorting.

Method	Ψ	Φ	Γ	SLL [dB]	D [dBi]	$HPBW$ [u]
Hilbert Sorting	1.36×10^{-2}	3.79×10^{-2}	1.46×10^{-1}	-15.57	10.89	1.20×10^{-1}
K-Means	1.38×10^{-2}	3.85×10^{-2}	1.15×10^{-1}	16.26	10.87	1.24×10^{-1}

Table IV: *Cosecant Squared* ($N = 16$, $Q = 6$): values of excitation matching index, Ψ , the field matching index, Φ , the power pattern matching index, Γ , the SLL, the directivity D and the half power beamwidth $HPBW$ obtained with Hilbert Sorting + ES and with the K-means.

Number elements $N = 18$, Number Clusters $Q = 6$

- difference excitation matching: $\Delta\Psi = -3.76 \times 10^{-4}$
- difference field matching: $\Delta\Phi = -9.49 \times 10^{-4}$
- difference power pattern matching: $\Delta\Gamma = 1.18 \times 10^{-3}$

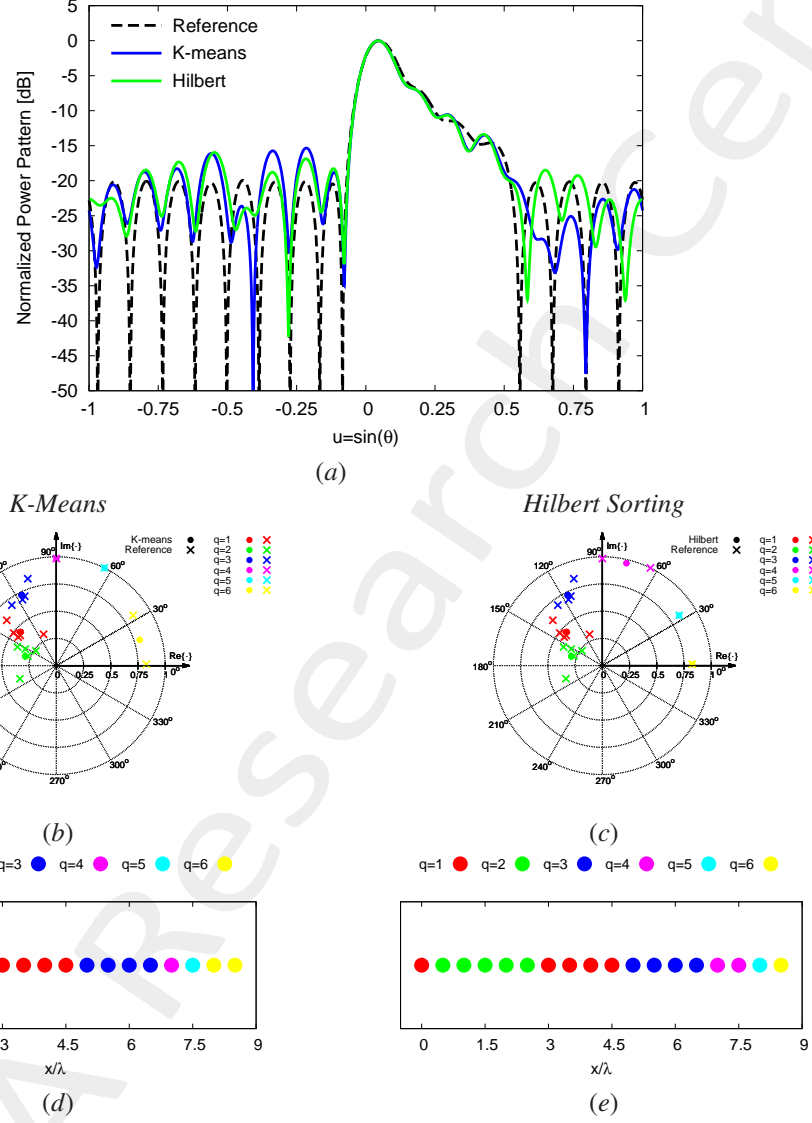


Figure 7: *Cosecant Squared* ($N = 18$, $Q = 6$): plot of (a) the power pattern of the clusterized solutions computed with the K-Means (blue line) and the Hilbert Sorting (green line) together with the reference ones (dashed black line), (b)(c) representation of the reference and the sub-array excitations in the complex plane, and (d)(e) layout of the clustered array synthetized with (b)(d) the K-means and (c)(e) the Hilbert Sorting.

Method	Ψ	Φ	Γ	SLL [dB]	D [dBi]	$HPBW$ [u]
Hilbert Sorting	1.67×10^{-2}	4.23×10^{-2}	1.20×10^{-1}	-15.96	11.11	1.11×10^{-1}
K-Means	1.71×10^{-2}	4.33×10^{-2}	1.19×10^{-1}	-15.34	11.12	1.10×10^{-1}

Table V: *Cosecant Squared* ($N = 18$, $Q = 6$): values of excitation matching index, Ψ , the field matching index, Φ , the power pattern matching index, Γ , the SLL, the directivity D and the half power beamwidth $HPBW$ obtained with Hilbert Sorting + ES and with the K-means.

Number elements $N = 19$, **Number Clusters** $Q = 6$

- difference excitation matching: $\Delta\Psi = -1.24 \times 10^{-3}$
- difference field matching: $\Delta\Phi = -3.88 \times 10^{-3}$
- difference power pattern matching: $\Delta\Gamma = -4.47 \times 10^{-2}$

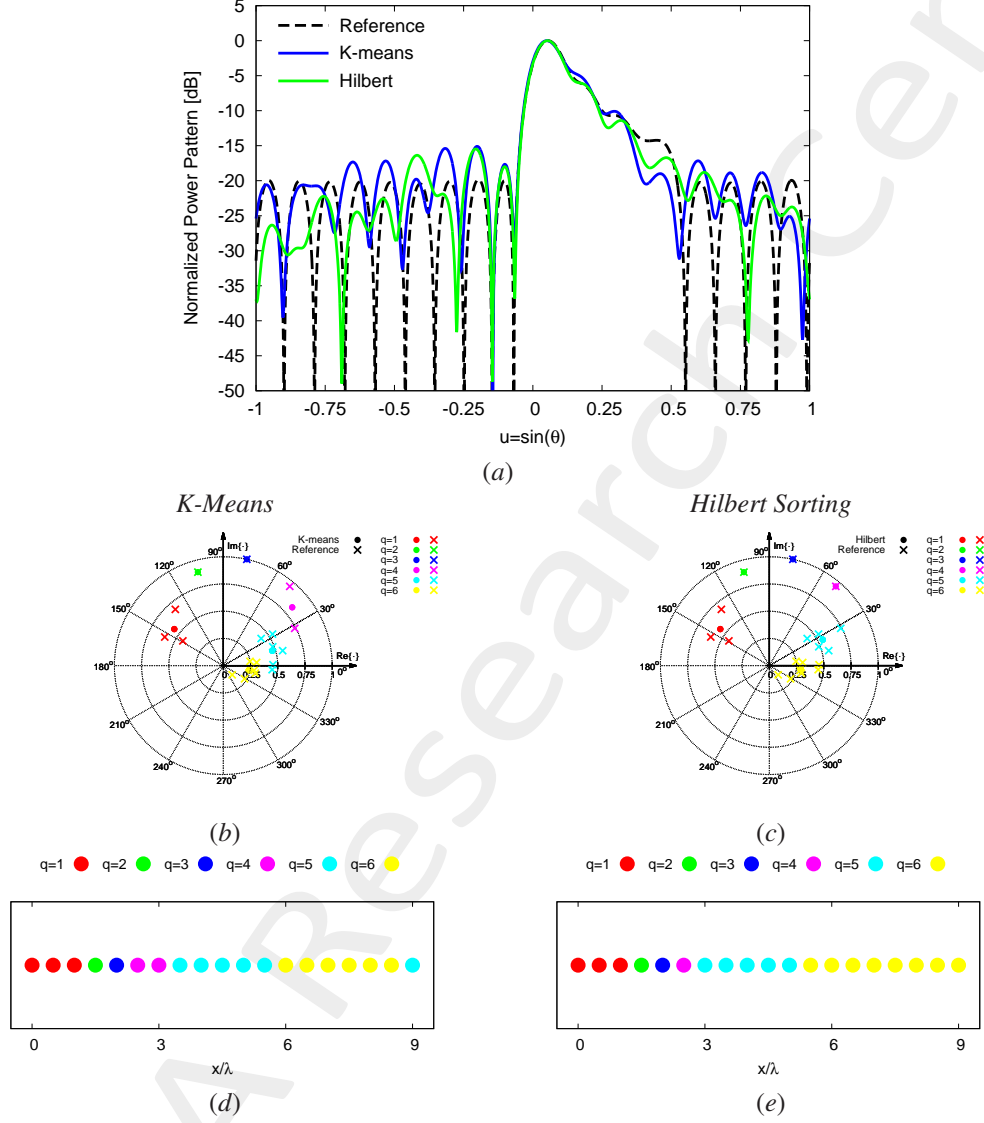


Figure 8: *Cosecant Squared* ($N = 19$, $Q = 6$): plot of (a) the power pattern of the clusterized solutions computed with the K-Means (blue line) and the Hilbert Sorting (green line) together with the reference ones (dashed black line), (b)(c) representation of the reference and the sub-array excitations in the complex plane, and (d)(e) layout of the clustered array synthetized with (b)(d) the K-means and (c)(e) the Hilbert Sorting.

Method	Ψ	Φ	Γ	SLL [dB]	D [dBi]	$HPBW$ [u]
Hilbert Sorting	1.45×10^{-2}	4.93×10^{-2}	9.96×10^{-2}	-15.47	11.24	1.08×10^{-1}
K-Means	1.57×10^{-2}	4.92×10^{-2}	1.44×10^{-1}	-15.10	10.92	1.16×10^{-1}

Table VI: *Cosecant Squared* ($N = 19$, $Q = 6$): values of excitation matching index, Ψ , the field matching index, Φ , the power pattern matching index, Γ , the SLL, the directivity D and the half power beamwidth $HPBW$ obtained with Hilbert Sorting + ES and with the K-means.

Number elements $N = 23$, **Number Clusters** $Q = 5$

- difference excitation matching: $\Delta\Psi = -7.73 \times 10^{-4}$
- difference field matching: $\Delta\Phi = -2.44 \times 10^{-3}$
- difference power pattern matching: $\Delta\Gamma = -3.61 \times 10^{-3}$

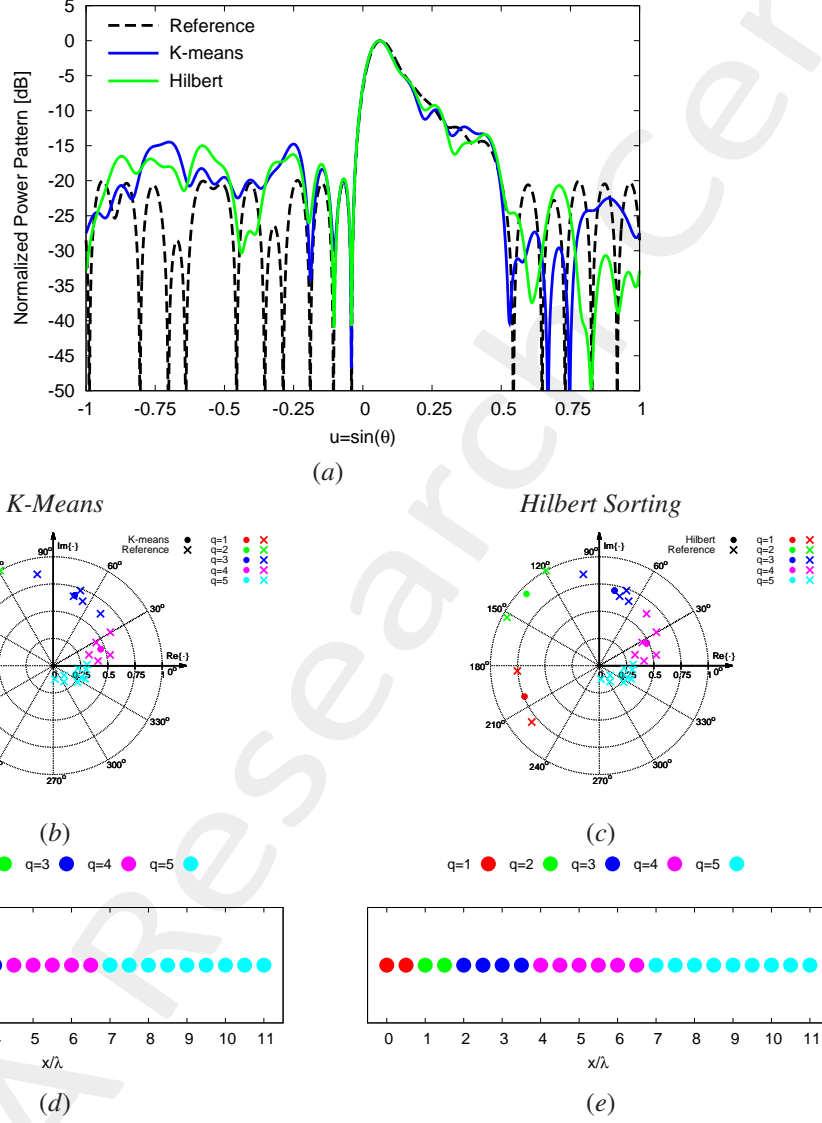


Figure 9: *Cosecant Squared* ($N = 23$, $Q = 5$): plot of (a) the power pattern of the clusterized solutions computed with the K-Means (blue line) and the Hilbert Sorting (green line) together with the reference ones (dashed black line), (b)(c) representation of the reference and the sub-array excitations in the complex plane, and (d)(e) layout of the clustered array synthetized with (b)(d) the K-means and (c)(e) the Hilbert Sorting.

Method	Ψ	Φ	Γ	SLL [dB]	D [dBi]	$HPBW$ [u]
Hilbert Sorting	3.05×10^{-2}	9.53×10^{-2}	2.11×10^{-1}	-15.00	11.50	9.50×10^{-2}
K-Means	3.13×10^{-2}	9.77×10^{-2}	2.15×10^{-1}	-14.47	11.49	9.58×10^{-2}

Table VII: *Cosecant Squared* ($N = 23$, $Q = 5$): values of excitation matching index, Ψ , the field matching index, Φ , the power pattern matching index, Γ , the SLL , the directivity D and the half power beamwidth $HPBW$ obtained with Hilbert Sorting + ES and with the K-means.

Number elements $N = 25$, **Number Clusters** $Q = 5$

- difference excitation matching: $\Delta\Psi = -1.14 \times 10^{-4}$
- difference field matching: $\Delta\Phi = -4.01 \times 10^{-4}$
- difference power pattern matching: $\Delta\Gamma = -8.28 \times 10^{-2}$

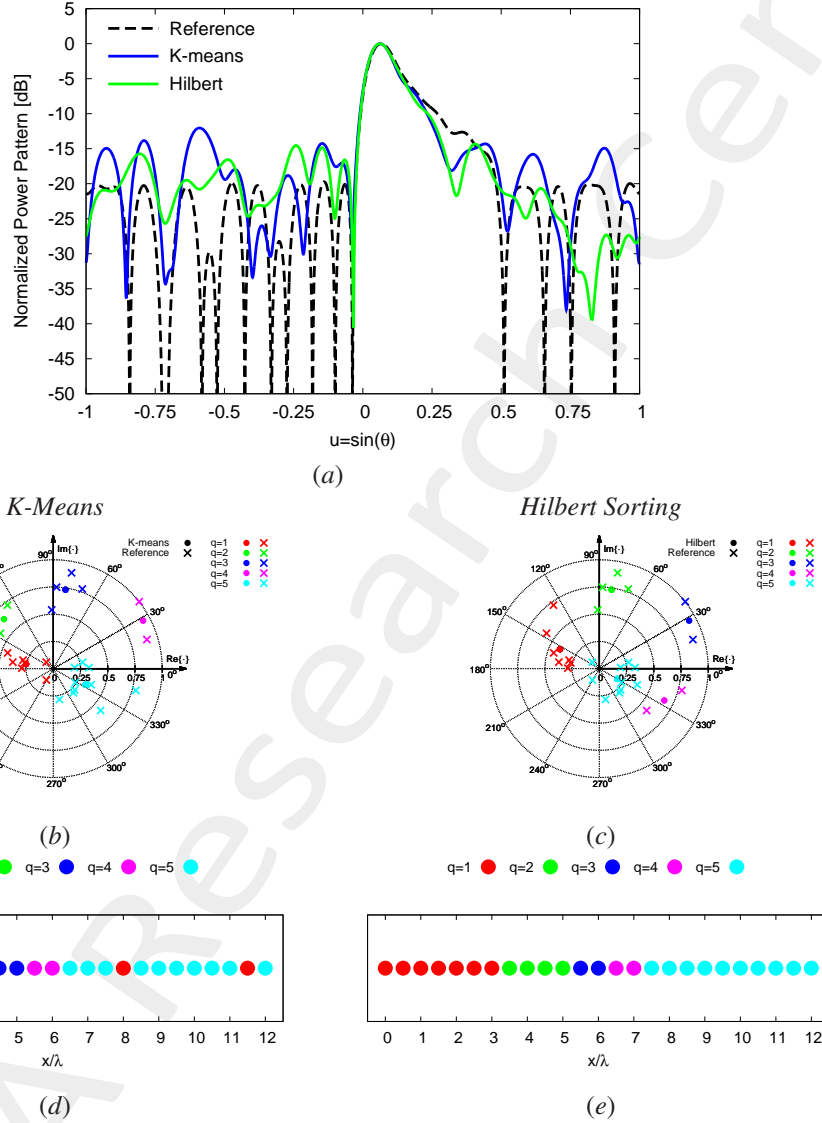


Figure 10: *Cosecant Squared* ($N = 25$, $Q = 5$): plot of (a) the power pattern of the clusterized solutions computed with the K-Means (blue line) and the Hilbert Sorting (green line) together with the reference ones (dashed black line), (b)(c) representation of the reference and the sub-array excitations in the complex plane, and (d)(e) layout of the clustered array synthetized with (b)(d) the K-means and (c)(e) the Hilbert Sorting.

Method	Ψ	Φ	Γ	SLL [dB]	D [dBi]	$HPBW$ [u]
Hilbert Sorting	3.47×10^{-2}	1.21×10^{-1}	2.35×10^{-1}	-14.54	11.68	9.86×10^{-2}
K-Means	3.48×10^{-2}	1.22×10^{-1}	3.18×10^{-1}	-12.04	11.37	9.57×10^{-2}

Table VIII: *Cosecant Squared* ($N = 25$, $Q = 5$): values of excitation matching index, Ψ , the field matching index, Φ , the power pattern matching index, Γ , the SLL, the directivity D and the half power beamwidth $HPBW$ obtained with Hilbert Sorting + ES and with the K-means.

1.1.3 Hibert Curve Sorting + Exhaustive Search (Excitation Matching): Comparison

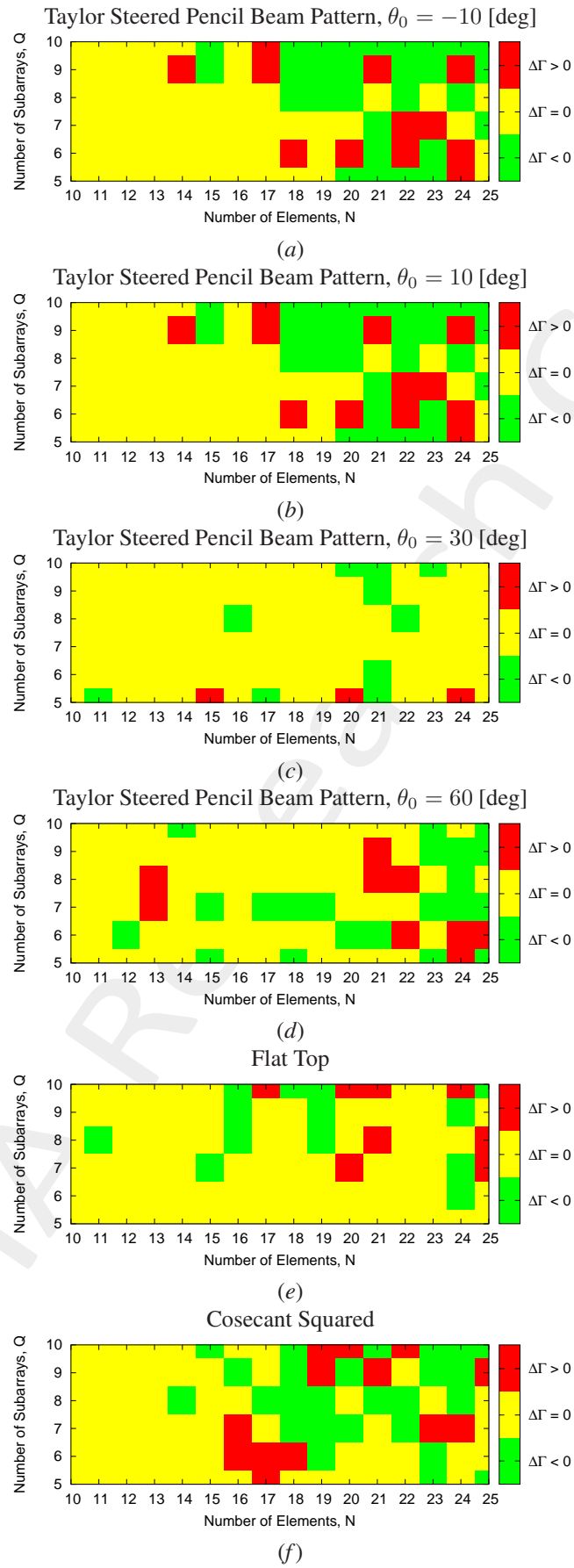


Figure 11: Performance Evaluation - Differential Power Pattern Matching, $\Delta\Gamma$ - 3 colors map: (a) Taylor Steered Pencil Beam Pattern, $\theta_0 = -10$ [deg], (b) Taylor Steered Pencil Beam Pattern, $\theta_0 = 10$ [deg], (c) Taylor Steered Pencil Beam Pattern, $\theta_0 = 30$ [deg], (d) Taylor Steered Pencil Beam Pattern, $\theta_0 = 60$ [deg], (e) Flat Top and (f) Cosecant Squared.

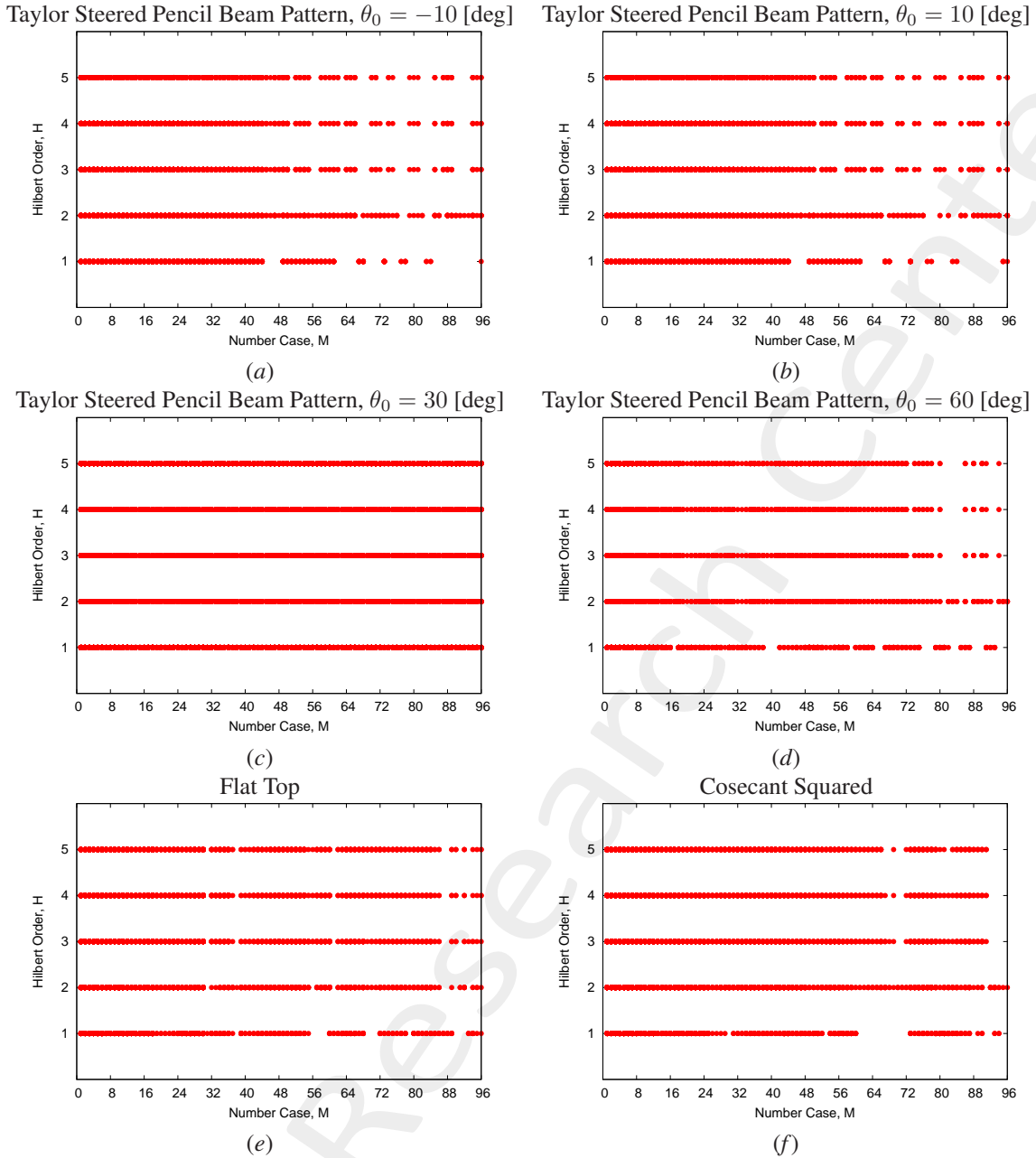


Figure 12: *Performance Evaluation - Differential Power Pattern Matching, $\Delta\Gamma$ - Hilbert Orders Analysis:* values of Hilbert for which the best performance is reached: (a) Taylor Steered Pencil Beam Pattern, $\theta_0 = -10$ [deg], (b) Taylor Steered Pencil Beam Pattern, $\theta_0 = 10$ [deg], (c) Taylor Steered Pencil Beam Pattern, $\theta_0 = 30$ [deg], (d) Taylor Steered Pencil Beam Pattern, $\theta_0 = 60$ [deg], (e) Flat Top and (f) Cosecant Squared.

Observation: Analysing the Hilbert order for which the best performance are reached, it can be deduced that for Hilbert Order $H = 2$, the proposed method gives the best results.

	Taylor Steered Pencil Beam Pattern				Shaped Beam Pattern	
$\Delta\Gamma$ evaluation	$\theta_0 = -10$ [deg]	$\theta_0 = 10$ [deg]	$\theta_0 = 30$ [deg]	$\theta_0 = 60$ [deg]	Flat Top	Cosecant Squared
# cases	96	96	96	96	96	96
# green ($\Delta\Gamma < 0$)	29	29	10	21	13	26
# yellow ($\Delta\Gamma = 0$)	55	55	83	66	75	57
# red ($\Delta\Gamma > 0$)	12	12	3	9	8	13

Table IX: *Performance Evaluation - Differential Power Pattern Matching (Hilbert Sorting + ES)*, $\Delta\Gamma$ - 3 colors map: evaluation number cases

	Taylor Steered Pencil Beam Pattern				Shaped Beam Pattern	
$\Delta\Gamma$ evaluation	$\theta_0 = -10$ [deg]	$\theta_0 = 10$ [deg]	$\theta_0 = 30$ [deg]	$\theta_0 = 60$ [deg]	Flat Top	Cosecant Squared
# cases	96	96	96	96	96	96
green $\Delta\Gamma$	9.14×10^{-3}	8.95×10^{-3}	1.43×10^{-2}	2.02×10^{-2}	1.96×10^{-2}	2.13×10^{-2}
yellow $\Delta\Gamma$	1.63×10^{-7}	1.67×10^{-7}	2.66×10^{-7}	2.09×10^{-7}	1.55×10^{-7}	1.23×10^{-7}
red $\Delta\Gamma$	4.23×10^{-3}	4.23×10^{-3}	1.57×10^{-2}	2.13×10^{-2}	1.35×10^{-2}	1.08×10^{-2}

Table X: *Performance Evaluation - Differential Power Pattern Matching means (Hilbert Sorting + ES)*, $\Delta\Gamma$ - 3 colors map: evaluation mean differential value $\Delta\Gamma$ for each case ($\Delta\Gamma < 0$, $\Delta\Gamma = 0$, $\Delta\Gamma > 0$)

1.1.4 Hibert Sorting + Exhaustive Search (Pattern Matching) vs K-means (Best Seed Excitation Matching)

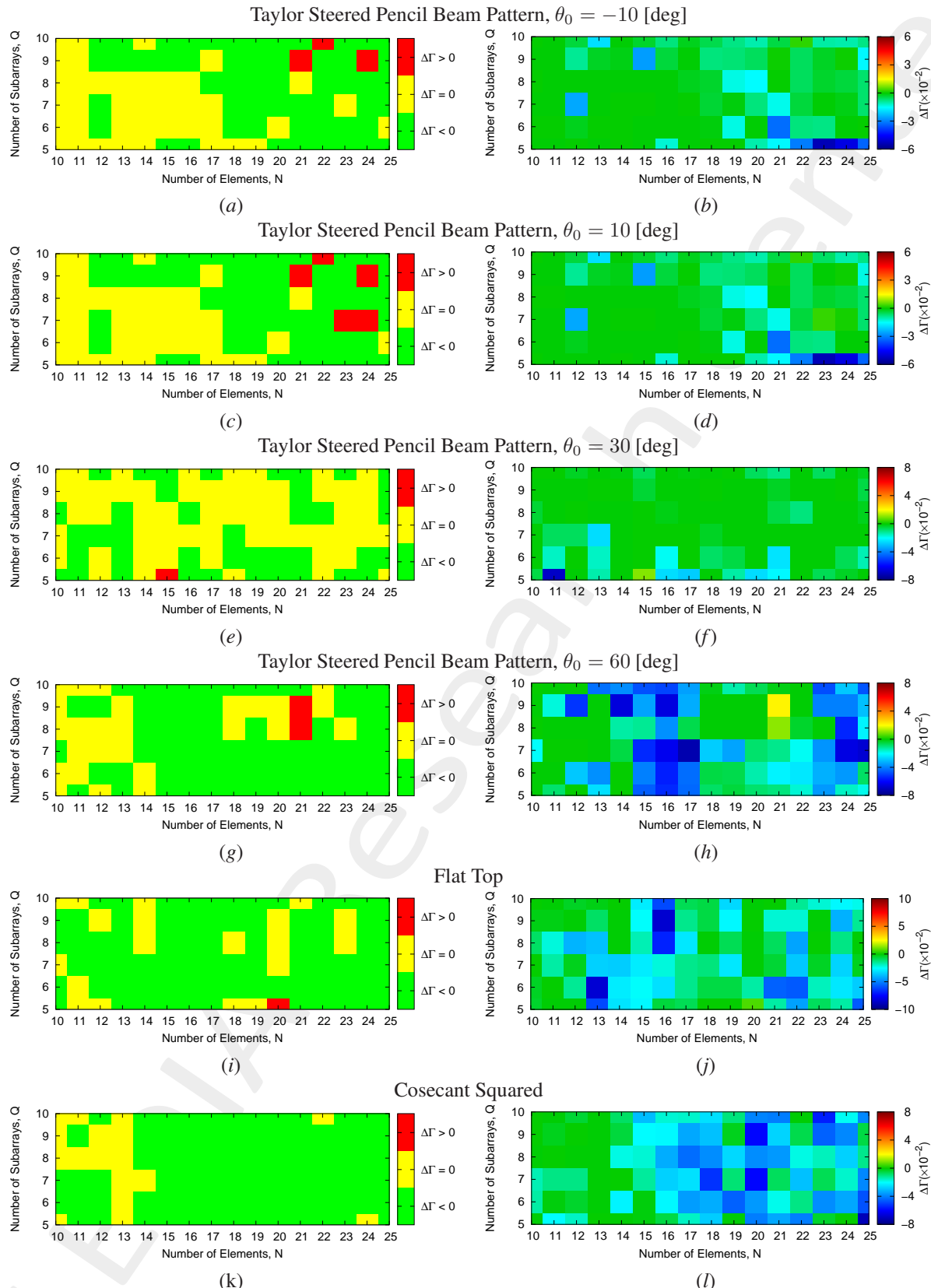


Figure 13: Performance Evaluation - Differential Power Pattern Matching, $\Delta\Gamma$ - 3 colors and nominal values map: (a)(b) Taylor Steered Pencil Beam Pattern, $\theta_0 = -10$ [deg], (c)(d) Taylor Steered Pencil Beam Pattern, $\theta_0 = 10$ [deg], (e)(f) Taylor Steered Pencil Beam Pattern, $\theta_0 = 30$ [deg], (g)(h) Taylor Steered Pencil Beam Pattern, $\theta_0 = 60$ [deg], (i)(j) Flat Top and (k)(l) Cosecant Squared.

	Taylor Steered Pencil Beam Pattern				Shaped Beam Pattern	
$\Delta\Gamma$ evaluation	$\theta_0 = -10$ [deg]	$\theta_0 = 10$ [deg]	$\theta_0 = 30$ [deg]	$\theta_0 = 60$ [deg]	Flat Top	Cosecant Squared
# cases	96	96	96	96	96	96
# green ($\Delta\Gamma < 0$)	54	53	40	68	76	79
# yellow ($\Delta\Gamma = 0$)	39	38	55	26	19	17
# red ($\Delta\Gamma > 0$)	3	5	1	2	1	0

Table XI: Performance Evaluation - Differential Power Pattern Matching (Hilbert Sorting + ES Pattern Matching), $\Delta\Gamma$ - 3 colors map: evaluation number cases

	Taylor Steered Pencil Beam Pattern				Shaped Beam Pattern	
$\Delta\Gamma$ evaluation	$\theta_0 = -10$ [deg]	$\theta_0 = 10$ [deg]	$\theta_0 = 30$ [deg]	$\theta_0 = 60$ [deg]	Flat Top	Cosecant Squared
# cases	96	96	96	96	96	96
green $\Delta\Gamma$	1.02×10^{-2}	1.02×10^{-2}	1.08×10^{-2}	2.94×10^{-2}	2.32×10^{-2}	2.36×10^{-2}
yellow $\Delta\Gamma$	5.51×10^{-8}	5.88×10^{-8}	6.37×10^{-8}	1.84×10^{-7}	3.21×10^{-8}	1.90×10^{-8}
red $\Delta\Gamma$	1.40×10^{-3}	1.61×10^{-3}	1.02×10^{-2}	1.62×10^{-2}	7.69×10^{-3}	//

Table XII: Performance Evaluation - Differential Power Pattern Matching means (Hilbert Sorting + ES Pattern Matching), $\Delta\Gamma$ - 3 colors map: evaluation mean differential value $\overline{\Delta\Gamma}$ for each case ($\Delta\Gamma < 0$, $\Delta\Gamma = 0$, $\Delta\Gamma > 0$)

In the following the comparison of the power pattern is reported for each test case evaluated. In particular, the ones with a major improvement compared to the K-means approach are shown.

Taylor Steered Pencil Beam Pattern, $\theta_0 = -10$ [deg]

- number elements: $N = 23$
- number clusters: $Q = 5$

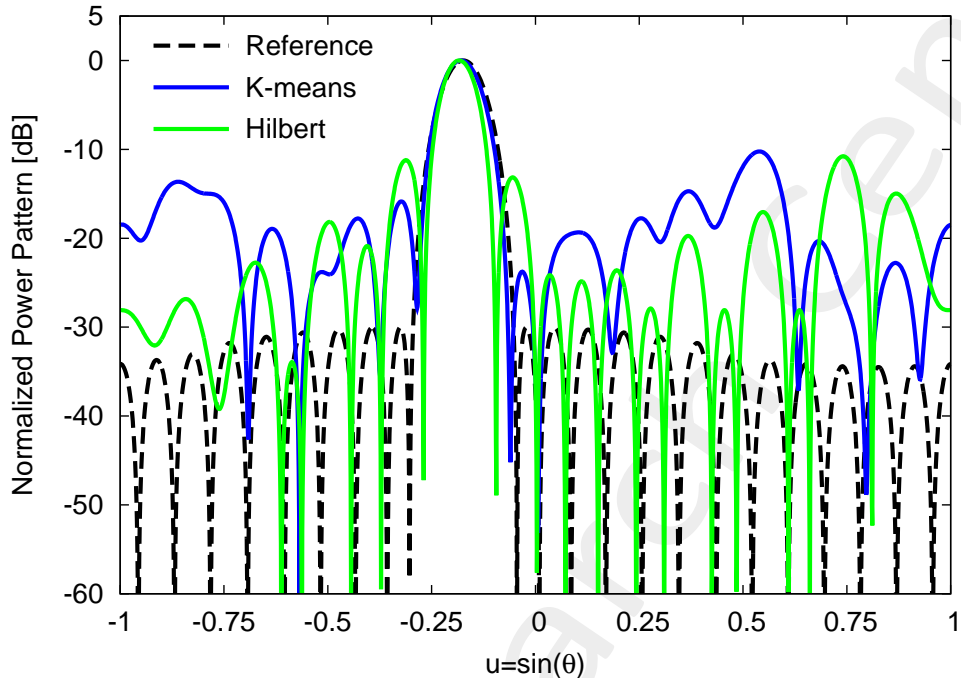


Figure 14: *Steered Pencil Beam* ($N = 23$, $Q = 5$, $\theta_0 = -10$ [deg]): power pattern of the clustered arrays synthetised with Hilbert+ES (Pattern Mathing), K-means together with the reference one.

<i>Method</i>	Γ
<i>Hilbert Sorting</i>	5.02×10^{-1}
<i>K-Means</i>	5.61×10^{-1}

Table XIII: *Steered Pencil Beam* ($N = 23$, $Q = 5$, $\theta_0 = -10$ [deg]): values of the power pattern matching index, Γ ,

Taylor Steered Pencil Beam Pattern, $\theta_0 = 10$ [deg]

- number elements: $N = 23$
- number clusters: $Q = 5$

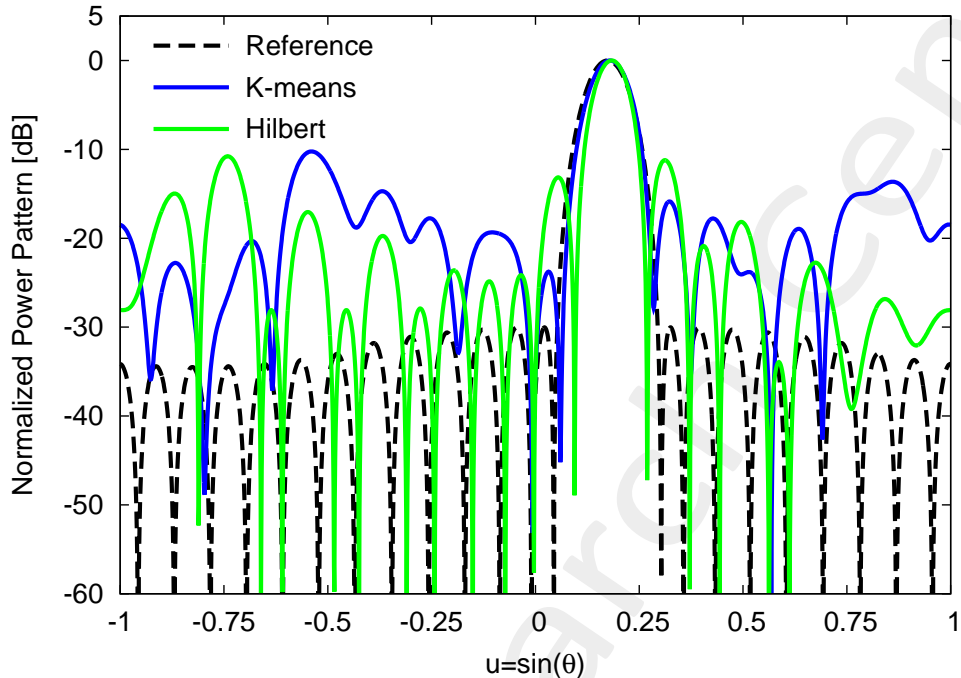


Figure 15: *Steered Pencil Beam* ($N = 23$, $Q = 5$, $\theta_0 = 10$ [deg]): power pattern of the clustered arrays synthetised with Hilbert+ES (Pattern Mathing), K-means together with the reference one.

<i>Method</i>	Γ
<i>Hilbert Sorting</i>	5.08×10^{-1}
<i>K-Means</i>	5.61×10^{-1}

Table XIV: *Steered Pencil Beam* ($N = 23$, $Q = 5$, $\theta_0 = 10$ [deg]): values of the power pattern matching index, Γ .

Taylor Steered Pencil Beam Pattern, $\theta_0 = 30$ [deg]

- number elements: $N = 17$
- number clusters: $Q = 5$

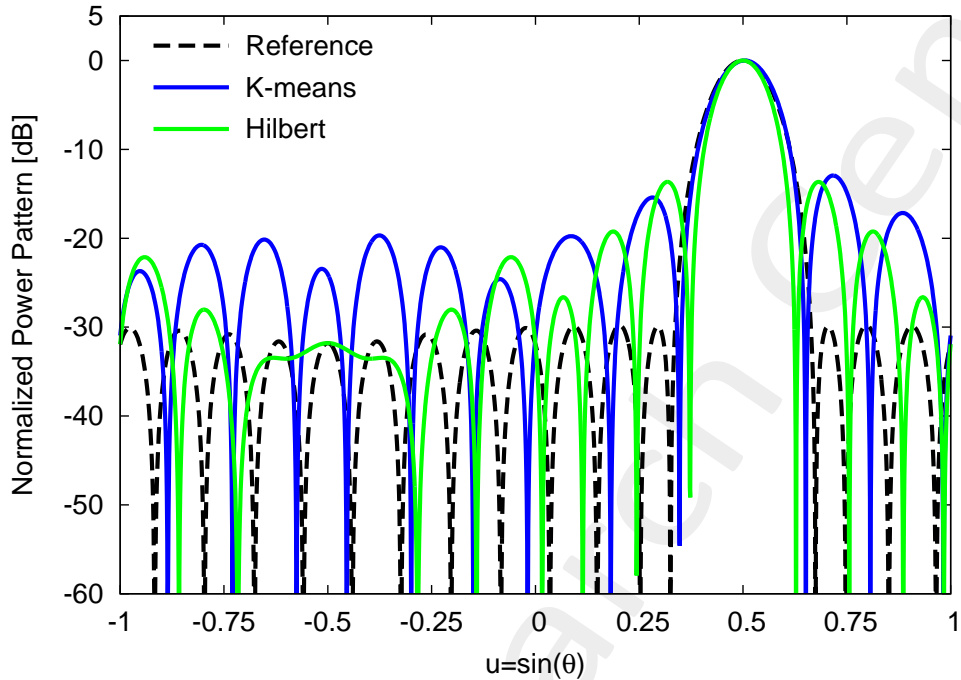


Figure 16: *Steered Pencil Beam* ($N = 17$, $Q = 5$, $\theta_0 = 30$ [deg]): power pattern of the clustered arrays synthetised with Hilbert+ES (Pattern Mathing), K-means together with the reference one.

Method	Γ
Hilbert Sorting	2.08×10^{-1}
K-Means	2.36×10^{-1}

Table XV: *Steered Pencil Beam* ($N = 17$, $Q = 5$, $\theta_0 = 30$ [deg]): values of the power pattern matching index, Γ .

Taylor Steered Pencil Beam Pattern, $\theta_0 = 60$ [deg]

- number elements: $N = 24$
- number clusters: $Q = 7$

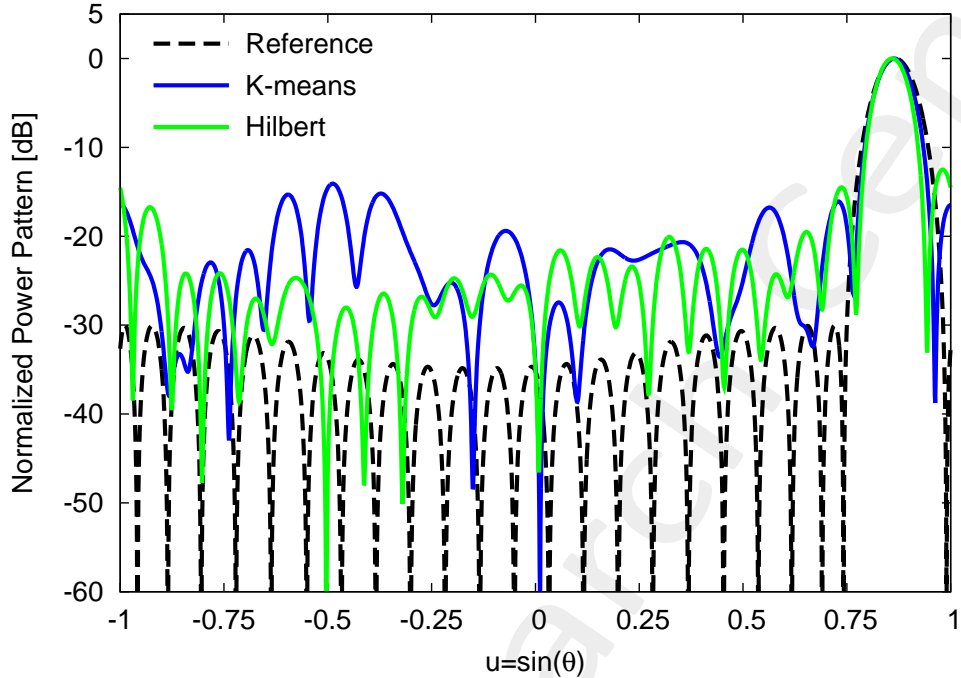


Figure 17: *Steered Pencil Beam* ($N = 24$, $Q = 7$, $\theta_0 = 60$ [deg]): power pattern of the clustered arrays synthetised with Hilbert+ES (Pattern Mathing), K-means together with the reference one.

<i>Method</i>	Γ
<i>Hilbert Sorting</i>	3.13×10^{-1}
<i>K-Means</i>	3.77×10^{-1}

Table XVI: *Steered Pencil Beam* ($N = 24$, $Q = 7$, $\theta_0 = 60$ [deg]): values of the power pattern matching index, Γ ,

Flat Top

- number elements: $N = 16$
- number clusters: $Q = 8$

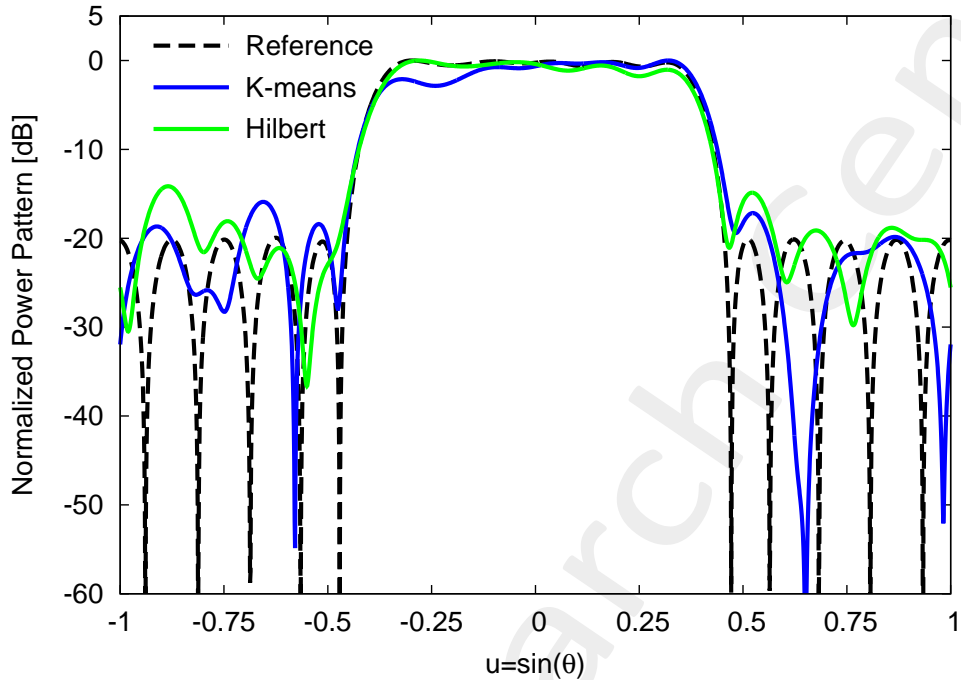


Figure 18: *Flat Top* ($N = 16$, $Q = 8$): power pattern of the clustered arrays synthetised with Hilbert+ES (Pattern Matching), K-means together with the reference one.

<i>Method</i>	Γ
<i>Hilbert Sorting</i>	9.44×10^{-2}
<i>K-Means</i>	1.62×10^{-1}

Table XVII: *Flat Top* ($N = 16$, $Q = 8$): values of the power pattern matching index, Γ .

Cosecant Squared

- number elements: $N = 16$
- number clusters: $Q = 8$

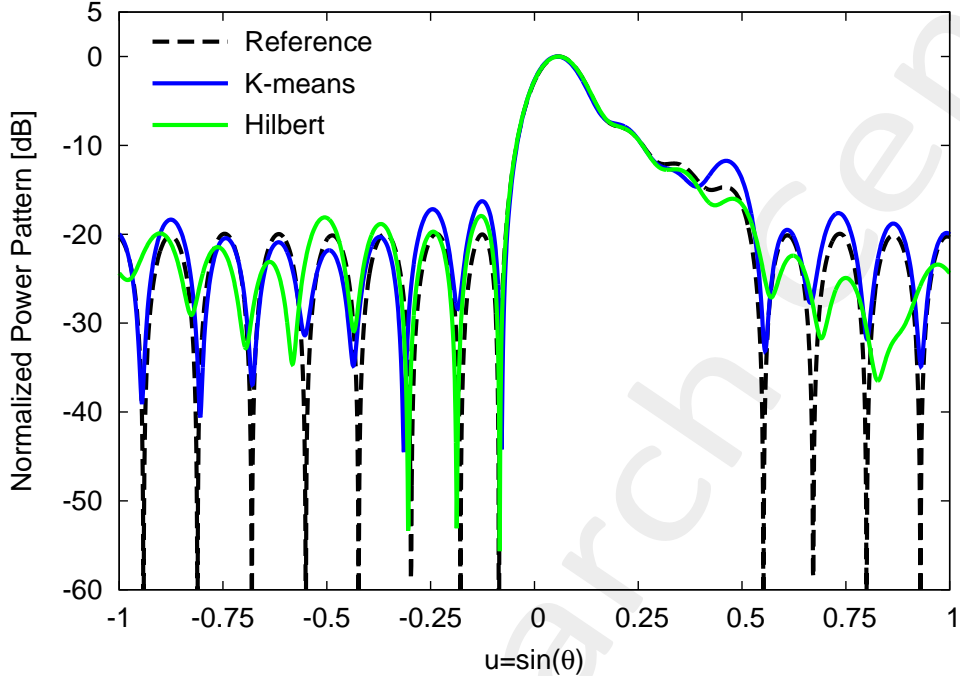


Figure 19: *Cosecant Squared* ($N = 16$, $Q = 8$): power pattern of the clustered arrays synthetised with Hilbert+ES (Pattern Matching), K-means together with the reference one.

<i>Method</i>	Γ
<i>Hilbert Sorting</i>	5.11×10^{-2}
<i>K-Means</i>	8.38×10^{-2}

Table XVIII: *Cosecant Squared* ($N = 16$, $Q = 8$): values of the power pattern matching index, Γ .

Observation

The comparison is not fair, since the best solution of the Hilbert Sorting approach has been obtained evaluating the pattern matching of all the possible contiguous partition of the given excitations list, while the best solution of the K-means is the best one in terms of excitations matching. However, there is no a relation linked the excitation and pattern matching, thus a solution with the a better excitation matching could has a worse pattern matching compared to another one.

To do a more fair comparison, it can be better to evaluate the pattern matching for all the random seeds used to initialize the K-means method.

1.1.5 Hibert Curve Sorting + Exhaustive Search (Pattern Matching) vs K-means (Best Seed Pattern Matching)

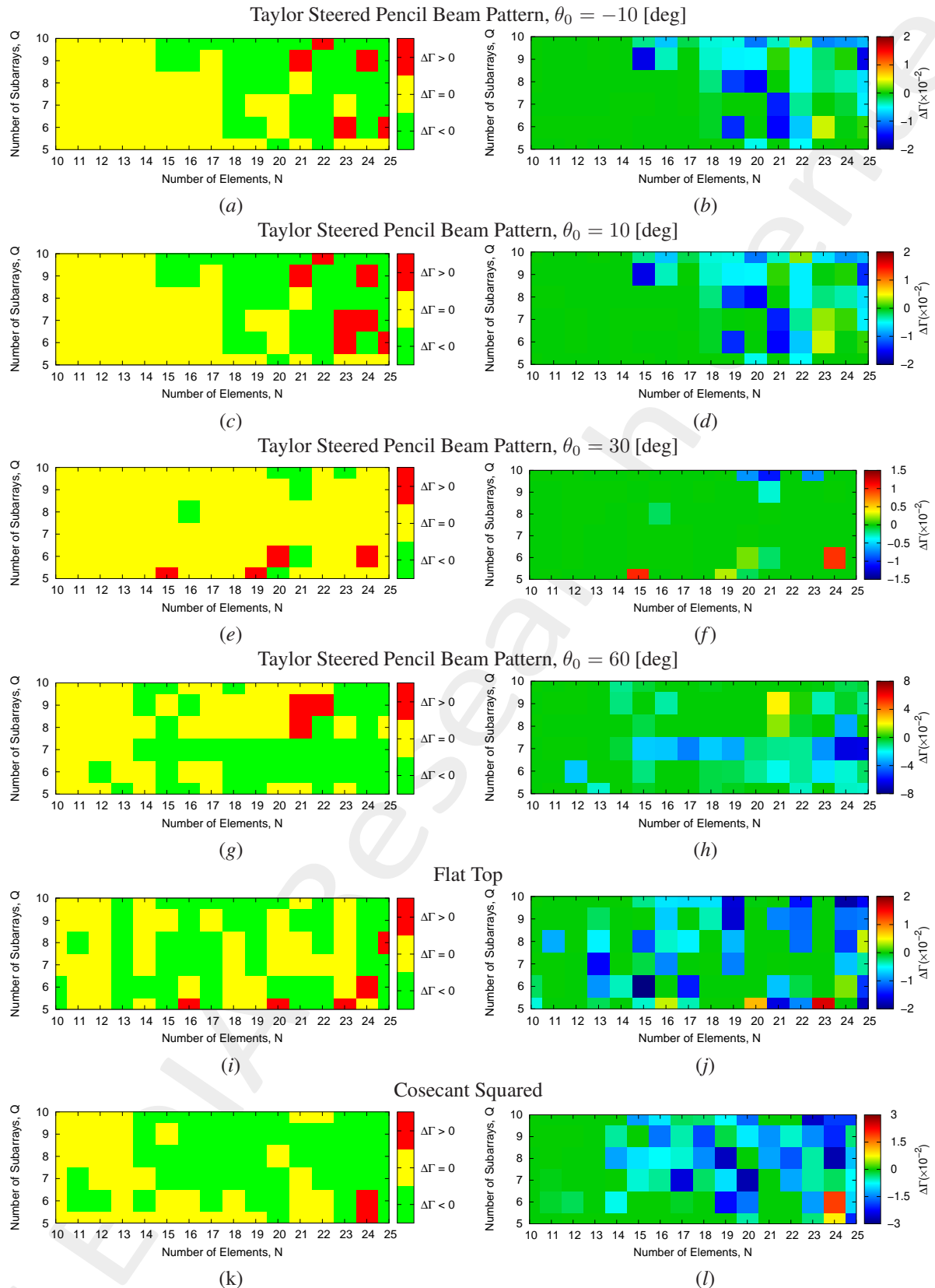


Figure 20: *Performance Evaluation - Differential Power Pattern Matching*, $\Delta\Gamma$ - 3 colors and nominal values map: (a)(b) Taylor Steered Pencil Beam Pattern, $\theta_0 = -10$ [deg], (c)(d) Taylor Steered Pencil Beam Pattern, $\theta_0 = 10$ [deg], (e)(f) Taylor Steered Pencil Beam Pattern, $\theta_0 = 30$ [deg], (g)(h) Taylor Steered Pencil Beam Pattern, $\theta_0 = 60$ [deg], (i)(j) Flat Top and (k)(l) Cosecant Squared.

	Taylor Steered Pencil Beam Pattern				Shaped Beam Pattern	
$\Delta\Gamma$ evaluation	$\theta_0 = -10$ [deg]	$\theta_0 = 10$ [deg]	$\theta_0 = 30$ [deg]	$\theta_0 = 60$ [deg]	Flat Top	Cosecant Squared
# cases	96	96	96	96	96	96
# green ($\Delta\Gamma < 0$)	37 [38.5 %]	36 [37.5 %]	7 [7.3 %]	44 [45.8 %]	49 [51.0 %]	54 [56.2 %]
# yellow ($\Delta\Gamma = 0$)	54 [56.2 %]	53 [55.2 %]	85 [88.5 %]	49 [51.0 %]	42 [43.8 %]	40 [41.8 %]
# red ($\Delta\Gamma > 0$)	5 [5.3 %]	7 [7.3 %]	4 [4.2 %]	3 [3.2 %]	5 [5.2 %]	2 [2.8 %]

Table XIX: Performance Evaluation - Differential Power Pattern Matching (Hilbert Sorting + ES Pattern Matching), $\Delta\Gamma$ - 3 colors map: evaluation number cases

	Taylor Steered Pencil Beam Pattern				Shaped Beam Pattern	
$\Delta\Gamma$ evaluation	$\theta_0 = -10$ [deg]	$\theta_0 = 10$ [deg]	$\theta_0 = 30$ [deg]	$\theta_0 = 60$ [deg]	Flat Top	Cosecant Squared
# cases	96	96	96	96	96	96
green $\Delta\Gamma$	6.37×10^{-3}	6.30×10^{-3}	4.52×10^{-3}	1.56×10^{-2}	8.11×10^{-3}	1.07×10^{-2}
yellow $\Delta\Gamma$	5.54×10^{-8}	5.19×10^{-8}	5.60×10^{-8}	2.21×10^{-7}	3.25×10^{-8}	2.96×10^{-8}
red $\Delta\Gamma$	1.81×10^{-3}	1.84×10^{-3}	6.06×10^{-3}	1.14×10^{-2}	6.82×10^{-3}	1.36×10^{-2}

Table XX: Performance Evaluation - Differential Power Pattern Matching means (Hilbert Sorting + ES Pattern Matching), $\Delta\Gamma$ - 3 colors map: evaluation mean differential value $\overline{\Delta\Gamma}$ for each case ($\Delta\Gamma < 0$, $\Delta\Gamma = 0$, $\Delta\Gamma > 0$)

In the following the comparison between patterns for the different cases considered.

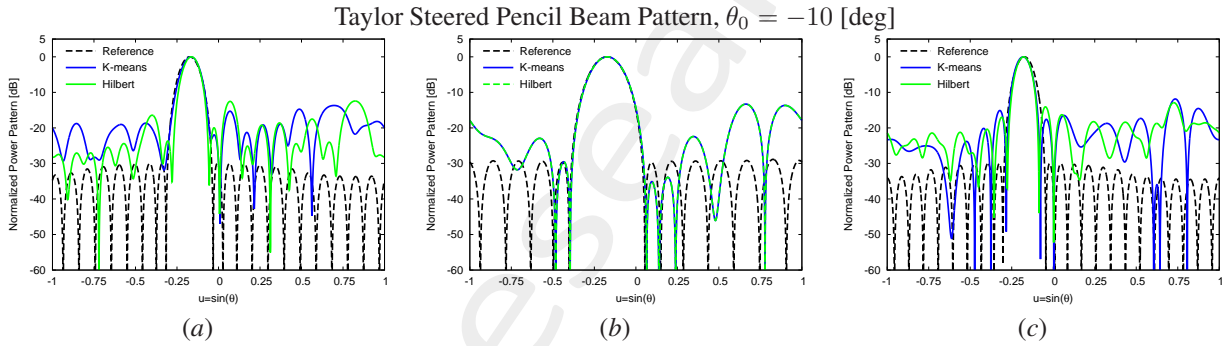


Figure 21: Taylor Steered Pencil Beam Pattern, $\theta_0 = -10$ [deg] - Power Pattern Comparison: (a) green case: $N = 21$, $Q = 6$ ($|\Delta\Gamma| = 1.49 \times 10^{-2}$), (b) yellow case: $N = 13$, $Q = 6$ ($|\Delta\Gamma| = 2.98 \times 10^{-8}$) and (c) red case: $N = 23$, $Q = 6$ ($|\Delta\Gamma| = 4.01 \times 10^{-3}$).

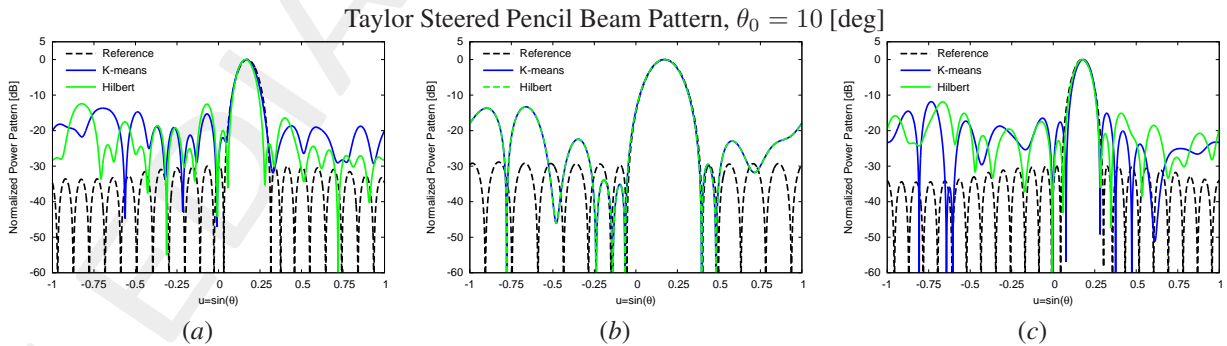


Figure 22: Taylor Steered Pencil Beam Pattern, $\theta_0 = 10$ [deg] - Power Pattern Comparison: (a) green case: $N = 21$, $Q = 6$ ($|\Delta\Gamma| = 1.49 \times 10^{-2}$), (b) yellow case: $N = 13$, $Q = 6$ ($|\Delta\Gamma| = 7.45 \times 10^{-8}$) and (c) red case: $N = 23$, $Q = 6$ ($|\Delta\Gamma| = 4.01 \times 10^{-3}$).

Taylor Steered Pencil Beam Pattern, $\theta_0 = 30$ [deg]

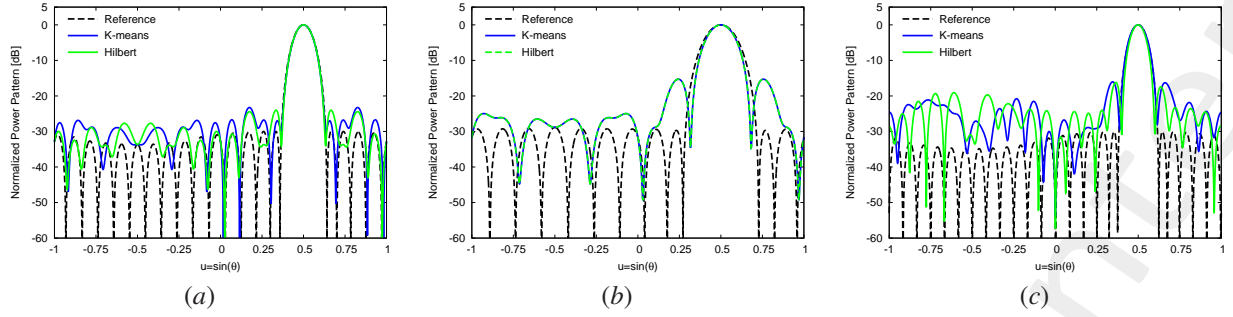


Figure 23: Taylor Steered Pencil Beam Pattern, $\theta_0 = 30$ [deg] - Power Pattern Comparison: (a) **green case**: $N = 21$, $Q = 10$ ($|\Delta\Gamma| = 1.26 \times 10^{-2}$), (b) **yellow case**: $N = 13$, $Q = 6$ ($|\Delta\Gamma| = 2.98 \times 10^{-8}$) and (c) **red case**: $N = 24$, $Q = 6$ ($|\Delta\Gamma| = 9.76 \times 10^{-3}$).

Taylor Steered Pencil Beam Pattern, $\theta_0 = 60$ [deg]

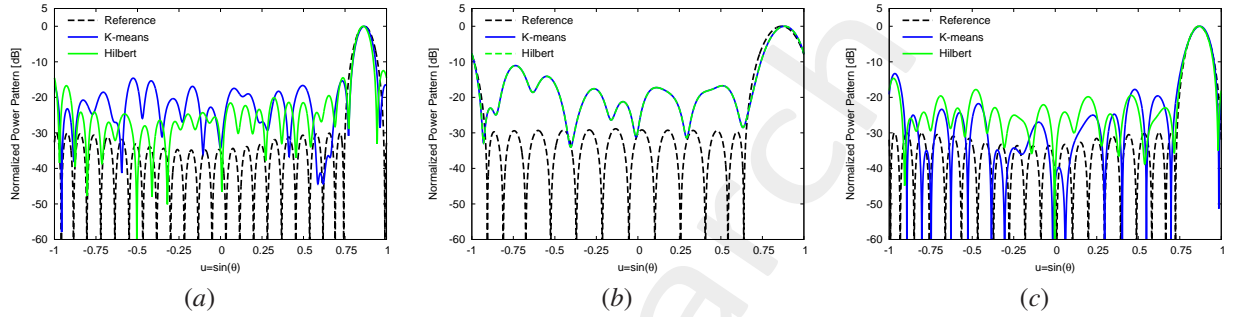


Figure 24: Taylor Steered Pencil Beam Pattern, $\theta_0 = 60$ [deg] - Power Pattern Comparison: (a) **green case**: $N = 24$, $Q = 7$ ($|\Delta\Gamma| = 6.41 \times 10^{-2}$), (b) **yellow case**: $N = 13$, $Q = 6$ ($|\Delta\Gamma| = 3.87 \times 10^{-7}$) and (c) **red case**: $N = 21$, $Q = 9$ ($|\Delta\Gamma| = 2.13 \times 10^{-2}$).

Flat Top

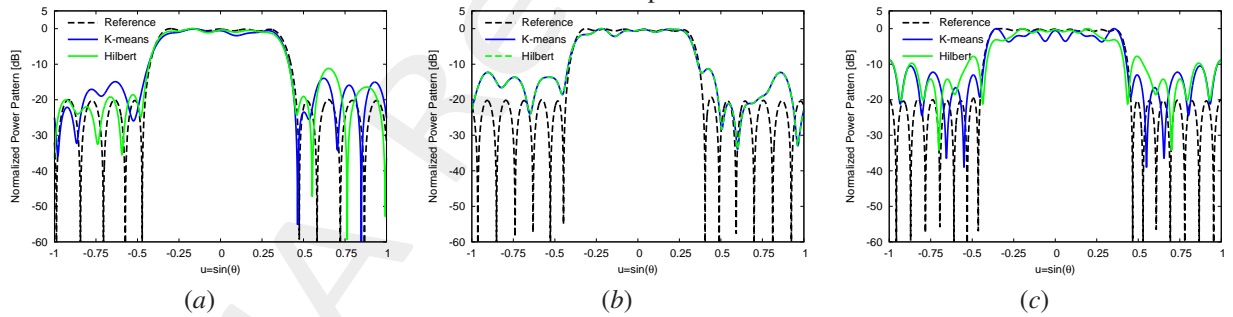


Figure 25: Flat Top - Power Pattern Comparison: (a) **green case**: $N = 15$, $Q = 6$ ($|\Delta\Gamma| = 2.20 \times 10^{-2}$), (b) **yellow case**: $N = 18$, $Q = 6$ ($|\Delta\Gamma| = 1.49 \times 10^{-8}$) and (c) **red case**: $N = 23$, $Q = 5$ ($|\Delta\Gamma| = 1.63 \times 10^{-2}$).

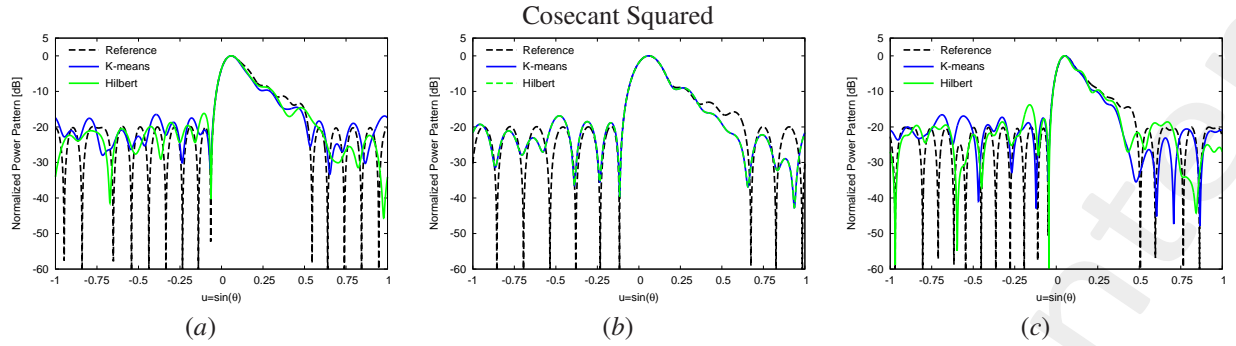


Figure 26: *Cosecant Squared - Power Pattern Comparison:* (a) **green case**: $N = 20, Q = 7$ ($|\Delta\Gamma| = 2.70 \times 10^{-2}$), (b) **yellow case**: $N = 13, Q = 6$ ($|\Delta\Gamma| = 4.84 \times 10^{-8}$) and (c) **red case**: $N = 24, Q = 6$ ($|\Delta\Gamma| = 1.89 \times 10^{-2}$).

1.1.6 Hibert Curve Sorting + Swap Element Algorithm: Comparison Pattern Matching (Cost Function: Excitation Matching)

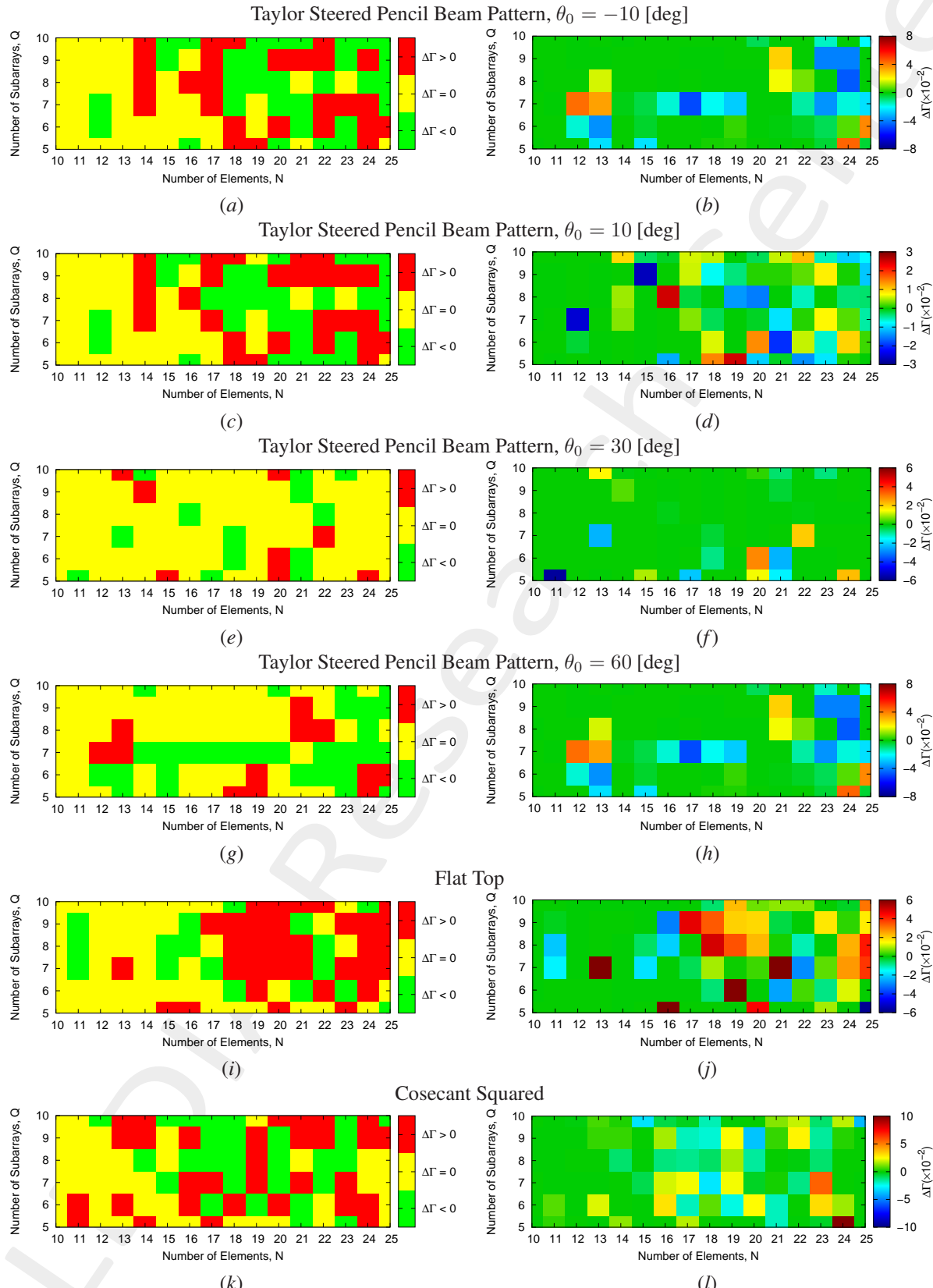


Figure 27: Performance Evaluation - Differential Power Pattern Matching, $\Delta\Gamma$ - 3 colors and nominal values map: (a)(b) Taylor Steered Pencil Beam Pattern, $\theta_0 = -10$ [deg], (c)(d) Taylor Steered Pencil Beam Pattern, $\theta_0 = 10$ [deg], (e)(f) Taylor Steered Pencil Beam Pattern, $\theta_0 = 30$ [deg], (g)(h) Taylor Steered Pencil Beam Pattern, $\theta_0 = 60$ [deg], (i)(j) Flat Top and (k)(l) Cosecant Squared.

	Taylor Steered Pencil Beam Pattern				Shaped Beam Pattern	
$\Delta\Gamma$ evaluation	$\theta_0 = -10$ [deg]	$\theta_0 = 10$ [deg]	$\theta_0 = 30$ [deg]	$\theta_0 = 60$ [deg]	Flat Top	Cosecant Squared
# cases	96	96	96	96	96	96
# green ($\Delta\Gamma < 0$)	31	30	13	29	17	27
# yellow ($\Delta\Gamma = 0$)	39	39	75	55	46	38
# red ($\Delta\Gamma > 0$)	26	27	8	12	33	31

Table XXI: *Performance Evaluation - Differential Power Pattern Matching (Hilbert Sorting + BEM)*, $\Delta\Gamma$ - 3 colors map: evaluation number cases

	Taylor Steered Pencil Beam Pattern				Shaped Beam Pattern	
$\Delta\Gamma$ evaluation	$\theta_0 = -10$ [deg]	$\theta_0 = 10$ [deg]	$\theta_0 = 30$ [deg]	$\theta_0 = 60$ [deg]	Flat Top	Cosecant Squared
# cases	96	96	96	96	96	96
green $\Delta\Gamma$	7.82×10^{-3}	7.85×10^{-3}	1.32×10^{-2}	1.73×10^{-2}	1.58×10^{-2}	1.50×10^{-2}
yellow $\Delta\Gamma$	1.75×10^{-7}	1.63×10^{-7}	2.66×10^{-7}	2.17×10^{-7}	1.54×10^{-7}	1.31×10^{-8}
red $\Delta\Gamma$	7.07×10^{-3}	6.84×10^{-3}	1.49×10^{-2}	2.05×10^{-2}	2.53×10^{-2}	1.83×10^{-2}

Table XXII: *Performance Evaluation - Differential Power Pattern Matching means (Hilbert Sorting + BEM)*, $\Delta\Gamma$ - 3 colors map: evaluation mean differential value $\overline{\Delta\Gamma}$ for each case ($\Delta\Gamma < 0$, $\Delta\Gamma = 0$, $\Delta\Gamma > 0$)

Observation

Using the Border Element Method to generate the clusters, a major number of $\Delta\Gamma > 0$ arises comparing with the use of the exhaustive search (excitation matching), this is due to the fact that the algorithm is not able to find the best solution in terms of excitation matching. However the BEM solution could result better than the K-means solution in terms of pattern matching.

More information on the topics of this document can be found in the following list of references.

References

- [1] N. Anselmi, L. Tosi, P. Rocca, G. Toso, and A. Massa, “A self-replicating single-shape tiling technique for the design of highly modular planar phased arrays - The case of L-shaped rep-tiles,” *IEEE Trans. Antennas Propag.*, vol. 71, no. 4, pp. 3335-3348, Apr. 2023.
- [2] A. Benoni, P. Rocca, N. Anselmi, and A. Massa, “Hilbert-ordering based clustering of complex-excitations linear arrays,” *IEEE Trans. Antennas Propag.*, vol. 70, no. 8, pp. 6751-6762, Aug. 2022.
- [3] P. Rocca, L. Poli, N. Anselmi, and A. Massa, “Nested optimization for the synthesis of asymmetric shaped beam patterns in sub-arrayed linear antenna arrays,” *IEEE Trans. Antennas Propag.*, vol. 70, no. 5, pp. 3385 - 3397, May 2022.
- [4] P. Rocca, L. Poli, A. Polo, and A. Massa, “Optimal excitation matching strategy for sub-arrayed phased linear arrays generating arbitrary shaped beams,” *IEEE Trans. Antennas Propag.*, vol. 68, no. 6, pp. 4638-4647, Jun. 2020.
- [5] G. Oliveri, G. Gottardi and A. Massa, “A new meta-paradigm for the synthesis of antenna arrays for future wireless communications,” *IEEE Trans. Antennas Propag.*, vol. 67, no. 6, pp. 3774-3788, Jun. 2019.
- [6] P. Rocca, M. H. Hannan, L. Poli, N. Anselmi, and A. Massa, “Optimal phase-matching strategy for beam scanning of sub-arrayed phased arrays,” *IEEE Trans. Antennas and Propag.*, vol. 67, no. 2, pp. 951-959, Feb. 2019.
- [7] N. Anselmi, P. Rocca, M. Salucci, and A. Massa, “Contiguous phase-clustering in multibeam-on-receive scanning arrays,” *IEEE Trans. Antennas Propag.*, vol. 66, no. 11, pp. 5879-5891, Nov. 2018.
- [8] L. Poli, G. Oliveri, P. Rocca, M. Salucci, and A. Massa, “Long-Distance WPT Unconventional Arrays Synthesis,” *J. Electromagn. Waves Appl. J.*, vol. 31, no. 14, pp. 1399-1420, Jul. 2017.
- [9] G. Gottardi, L. Poli, P. Rocca, A. Montanari, A. Aprile, and A. Massa, “Optimal Monopulse Beamforming for Side-Looking Airborne Radars,” *IEEE Antennas Wireless Propag. Lett.*, vol. 16, pp. 1221-1224, 2017.
- [10] G. Oliveri, M. Salucci, and A. Massa, “Synthesis of modular contiguously clustered linear arrays through a sparseness-regularized solver,” *IEEE Trans. Antennas Propag.*, vol. 64, no. 10, pp. 4277-4287, Oct. 2016.
- [11] P. Rocca, G. Oliveri, R. J. Mailloux, and A. Massa, “Unconventional phased array architectures and design Methodologies - A review,” *Proc. IEEE*, Invited Paper, vol. 104, no. 3, pp. 544-560, March 2016.
- [12] P. Rocca, M. D’Urso, and L. Poli, “Advanced strategy for large antenna array design with subarray-only amplitude and phase control,” *IEEE Antennas and Wireless Propag. Lett.*, vol. 13, pp. 91-94, 2014.
- [13] L. Manica, P. Rocca, G. Oliveri, and A. Massa, “Synthesis of multi-beam sub-arrayed antennas through an excitation matching strategy,” *IEEE Trans. Antennas Propag.*, vol. 59, no. 2, pp. 482-492, Feb. 2011.

-
- [14] G. Oliveri, "Multi-beam antenna arrays with common sub-array layouts," *IEEE Antennas Wireless Propag. Lett.*, vol. 9, pp. 1190-1193, 2010.
- [15] P. Rocca, R. Haupt, and A. Massa, "Sidelobe reduction through element phase control in sub-arrayed array antennas," *IEEE Antennas Wireless Propag. Lett.*, vol. 8, pp. 437-440, 2009.
- [16] P. Rocca, L. Manica, R. Azaro, and A. Massa, "A hybrid approach for the synthesis of sub-arrayed monopulse linear arrays," *IEEE Trans. Antennas Propag.*, vol. 57, no. 1, pp. 280-283, Jan. 2009.
- [17] L. Manica, P. Rocca, M. Benedetti, and A. Massa, "A fast graph-searching algorithm enabling the efficient synthesis of sub-arrayed planar monopulse antennas," *IEEE Trans. Antennas Propag.*, vol. 57, no. 3, pp. 652-664, Mar. 2009.
- [18] P. Rocca, L. Manica, A. Martini, and A. Massa, "Compromise sum-difference optimization through the iterative contiguous partition method," *IET Microwaves, Antennas & Propagation*, vol. 3, no. 2, pp. 348-361, 2009.
- [19] L. Manica, P. Rocca, and A. Massa, "An excitation matching procedure for sub-arrayed monopulse arrays with maximum directivity," *IET Radar, Sonar & Navigation*, vol. 3, no. 1, pp. 42-48, Feb. 2009.
- [20] L. Manica, P. Rocca, and A. Massa, "Design of subarrayed linear and planar array antennas with SLL control based on an excitation matching approach," *IEEE Trans. Antennas Propag.*, vol. 57, no. 6, pp. 1684-1691, Jun. 2009.
- [21] L. Manica, P. Rocca, A. Martini, and A. Massa, "An innovative approach based on a tree-searching algorithm for the optimal matching of independently optimum sum and difference excitations," *IEEE Trans. Antennas Propag.*, vol. 56, no. 1, pp. 58-66, Jan. 2008.
- [22] P. Rocca, L. Manica, and A. Massa, "An effective excitation matching method for the synthesis of optimal compromises between sum and difference patterns in planar arrays," *Progress in Electromagnetic Research B*, vol. 3, pp. 115-130, 2008.
- [23] P. Rocca, L. Manica, and A. Massa, "Directivity optimization in planar sub-arrayed monopulse antenna," *Progress in Electromagnetic Research L*, vol. 4, pp. 1-7, 2008.
- [24] P. Rocca, L. Manica, M. Pastorino, and A. Massa, "Boresight slope optimization of sub-arrayed linear arrays through the contiguous partition method," *IEEE Antennas Wireless Propag. Lett.*, vol. 8, pp. 253-257, 2008.
- [25] P. Rocca, L. Manica, and A. Massa, "Synthesis of monopulse antennas through the iterative contiguous partition method," *Electronics Letters*, vol. 43, no. 16, pp. 854-856, Aug. 2007.
- [26] P. Rocca, L. Manica, A. Martini, and A. Massa, "Synthesis of large monopulse linear arrays through a tree-based optimal excitations matching," *IEEE Antennas Wireless Propag. Lett.*, vol. 7, pp. 436-439, 2007.